

Water Resources Research®



RESEARCH ARTICLE

10.1029/2024WR037256

Key Points:

- We present a comprehensive data set of streamflow, groundwater levels and geophysics from an intermittent stream in semi-arid Australia
- Underlying streambed geological structures control streamflow intermittence, duration, and interactions with groundwater
- Combinations of geological controls create a “goldilocks zone” which likely maximizes components of the water balance in similar landscapes

Supporting Information:

Supporting Information may be found in the online version of this article.

Correspondence to:

E. Zarate,
emzar@bgs.ac.uk







Citation:

Zarate, E., Andersen, M. S., Rau, G. C., Acworth, R. I., Rutledge, H., MacDonald, A. M., & Cuthbert, M. O. (2025). How alluvial storage controls spatiotemporal water balance partitioning in intermittent and ephemeral stream systems. *Water Resources Research*, 61, e2024WR037256. <https://doi.org/10.1029/2024WR037256>

Received 31 JAN 2024

Accepted 20 FEB 2025

How Alluvial Storage Controls Spatiotemporal Water Balance Partitioning in Intermittent and Ephemeral Stream Systems

E. Zarate^{1,2} , M. S. Andersen^{3,4} , G. C. Rau^{4,5} , R. I. Acworth³ , H. Rutledge⁶,
A. M. MacDonald² , and M. O. Cuthbert^{1,3} 

¹School of Earth & Environmental Sciences, Cardiff University, Cardiff, UK, ²British Geological Survey, Lyell Centre, Edinburgh, UK, ³School of Civil and Environmental Engineering, The University of New South Wales (UNSW), Sydney, NSW, Australia, ⁴National Centre for Groundwater Research and Training (NCGRT), Bedford Park, SA, Australia, ⁵School of Environmental and Life Sciences, The University of Newcastle, Callaghan, NSW, Australia, ⁶School of Chemical Engineering, The University of New South Wales (UNSW), Sydney, NSW, Australia

Abstract The hydrological dynamics of intermittent rivers and ephemeral streams (IRES) impacts the availability of water to riparian ecosystems, the height of downstream runoff peaks, and the replenishment of groundwater systems. Despite its significance, the influence of superficial geology on IRES flow processes remains an area of limited understanding. Here we first present a comprehensive data set encompassing streamflow and groundwater levels from an intermittent stream situated in New South Wales, Australia. We then use targeted geophysical investigations to show how the configurations of superficial geology control the streamflow and groundwater responses. The analysis reveals that periods of stable stream stage consistently occur after episodic surges in streamflow, followed by recession and channel desiccation. The duration of the stable phases exhibits an upstream-to-downstream pattern, reaching a maximum of 44 ± 3 days upstream and then abruptly declining further downstream. There is remarkable consistency in the duration of these stable flow periods, irrespective of the size of preceding streamflow peaks. We propose two primary controls of this behavior: (a) variability in permeability contrasts between channel alluvium and surrounding geological deposits, and (b) longitudinal fluctuations in the volume of the recent channel alluvial reservoir. The interplay of these controls generates a “goldilocks zone,” which optimizes riparian water availability and the potential for groundwater recharge in IRES landscapes. These geological controls may reflect a continuum present in other dryland catchments with widespread implications for groundwater recharge and stream classification based on flow occurrence and duration.

Plain Language Summary Intermittent rivers and ephemeral streams provide water to plants and animals, influence downstream floods, and help refill underground water supplies. However, we don't fully understand how geology controls when and where water flows in these rivers. In this study, we examined an intermittent river in New South Wales, Australia, by measuring water levels in the river and underground. We also used specialized tools to study how layers of rocks and sediments influence water movement. Our results show that after heavy storms the water in the river rises quickly, then stays at a stable level before slowly drying up. These stable periods last the longest upstream—up to 44 days—but become shorter downstream. Surprisingly, the length of these stable periods is always the same, no matter how big the storm was or how high the river got. We found two key factors behind this: how much water the sand in the river can hold and how easily water moves between this sand and surrounding rocks. Together, these factors create an ideal zone that supports plant life and groundwater recharge. Understanding these patterns can help us manage water in dry areas and improve how these rivers are classified.

1. Introduction

Intermittent rivers and ephemeral streams (IRES) occur globally across all climates, with more than half of global channels drying periodically (Datry, Fritz, & Leigh, 2016; Datry, Pella, et al., 2016; Messenger et al., 2021). In drylands (arid, semi-arid and sub-humid regions), IRES are more widespread and comprise >80% of the channel network (Datry et al., 2011; Levick et al., 2008).

In both dryland and humid environments, IRES perform a variety of critical ecosystem services (Kaletová et al., 2019; Stubbington et al., 2020), including transport of biota, materials, nutrients, and water within the

© 2025. The Author(s).

This is an open access article under the terms of the [Creative Commons Attribution License](https://creativecommons.org/licenses/by/4.0/), which permits use, distribution and reproduction in any medium, provided the original work is properly cited.

landscape (Acuña et al., 2017; Alan Yeakley et al., 2016; Datry et al., 2017) and host diverse aquatic and riparian ecosystems (Datry, Fritz, & Leigh, 2016; Datry, Pella, et al., 2016; Katz et al., 2012). Ephemeral streamflow is often the primary source of surface water to these ecosystems (Stromberg & Merritt, 2016) and is crucial in maintaining their ecological health and diversity (Labbe & Fausch, 2000; Saccò et al., 2021). Due to its widespread distribution and relative resilience to climate variability, groundwater is often the only viable source of freshwater in dryland regions (Dai, 2013; Feng & Fu, 2013; Huang et al., 2016) and streamflow infiltration via the beds of ephemeral streams is a key pathway for replenishment of groundwater recharge (Cuthbert et al., 2019; Keppel & Renard, 1962; Wheeler, 2008).

Demands on dryland water resources are being intensified by rising population (DESA, 2017), human activity (Chen et al., 2019; Wada et al., 2013) and climate change (Abel et al., 2020; Berdugo et al., 2020; Huang et al., 2017; Taylor, Scanlon, et al., 2013; Taylor, Todd, et al., 2013). Consequently, it is crucial to improve our understanding of the water balance partitioning (i.e., the partitioning between streamflow, infiltration, evapotranspiration, groundwater recharge and water extractions). Additionally, understanding the sensitivity of this partitioning to environmental change is essential for the sustainable management of dryland water resources in the future (Gleeson et al., 2020; Keshavarzi et al., 2017; Meixner et al., 2016).

However, assessing the water balance in dryland IRES has proven to be difficult. Many of the common methods used for monitoring and data collection in perennial river systems are not appropriate in dryland IRES, where monitoring infrastructure (if present) often fails or is destroyed due to the flashy and extreme nature of runoff events (Acworth et al., 2016; El Khalki et al., 2020; Pilgrim et al., 1988; Shanafield et al., 2021). These challenges have slowed the development and understanding of the physical processes that underpin the various fluxes and interactions between surface water and groundwater in drylands (Cuthbert et al., 2019; Green et al., 2011).

While several studies that have linked the role of topography (Ward et al., 2018; Warix et al., 2021), vegetation (Warix et al., 2023) and anthropogenic factors (Fuchs et al., 2019; Zipper et al., 2022) in mediating streamflow in IRES, the configuration of superficial geology surrounding these systems in drylands has also been shown to play a crucial role in controlling the variability in their water balance partitioning (Zarate et al., 2021). In dryland IRES, marked temporal and spatial variability in the hydraulic conductivities of alluvial deposits can provide controls on surface water-groundwater interactions (Costa et al., 2013; Dahan et al., 2008; Flinchum et al., 2020; McCallum et al., 2014). Underlying geology can control hydrologic flow paths, the depth of alluvial deposits (Owen & Dahlin, 2005), the locations of groundwater outflow to streams (Harrington et al., 2014) and the groundwater recharge in these regions (Dvory et al., 2016; Goodrich et al., 2018). Yet the geological controls on water balance partitioning in these contexts are still poorly understood (Cuthbert et al., 2016).

This paper aims to (a) quantify variations in subsurface geology, stream stage and groundwater levels along an intermittent stream system using an unusually rich monitoring site in the Maules Creek Catchment (New South Wales, Australia); (b) elucidate how configurations of superficial geology surrounding the stream control the variability in water balance partitioning; and (c) generate a conceptual model of water balance partitioning in IRES with varying geology that is applicable to a wide range of dryland settings. Our results help understand the consequence of changes to surface water-groundwater interactions (such as from river regulation, groundwater extractions and climate change) on water resources in drylands. This study also demonstrates the benefits of linking hydrological data with geophysical imaging to better understand flow paths through superficial and surrounding deposits that can be widely applied to other areas.

2. Methods

2.1. Site Description and Geology

The Maules Creek catchment is a semi-arid sub-catchment of the Namoi River in New South Wales, Australia (Figure 1a). The catchment has been described in detail in previous studies (M. S. Andersen & Acworth, 2009; Cuthbert et al., 2016; McCallum et al., 2013; Rau et al., 2010, 2017) and is only briefly summarized here. The catchment has a surface area of approximately 1,100 km² (study area in black line, Figure 1b) and is located on the western slopes of the Great Dividing Range, south-east of the township of Narrabri. It is bounded to the east by the New England Fold Belt and the Great Dividing Range, to the north by the Nandewar Range (and Mount Kaputar), to the south by the Leard State Forest and Gins Leap Gap, and to the west by a low ridge of hills that represent the edge of the Great Artesian Basin sediments. Middle Creek is an intermittent tributary that drains approximately

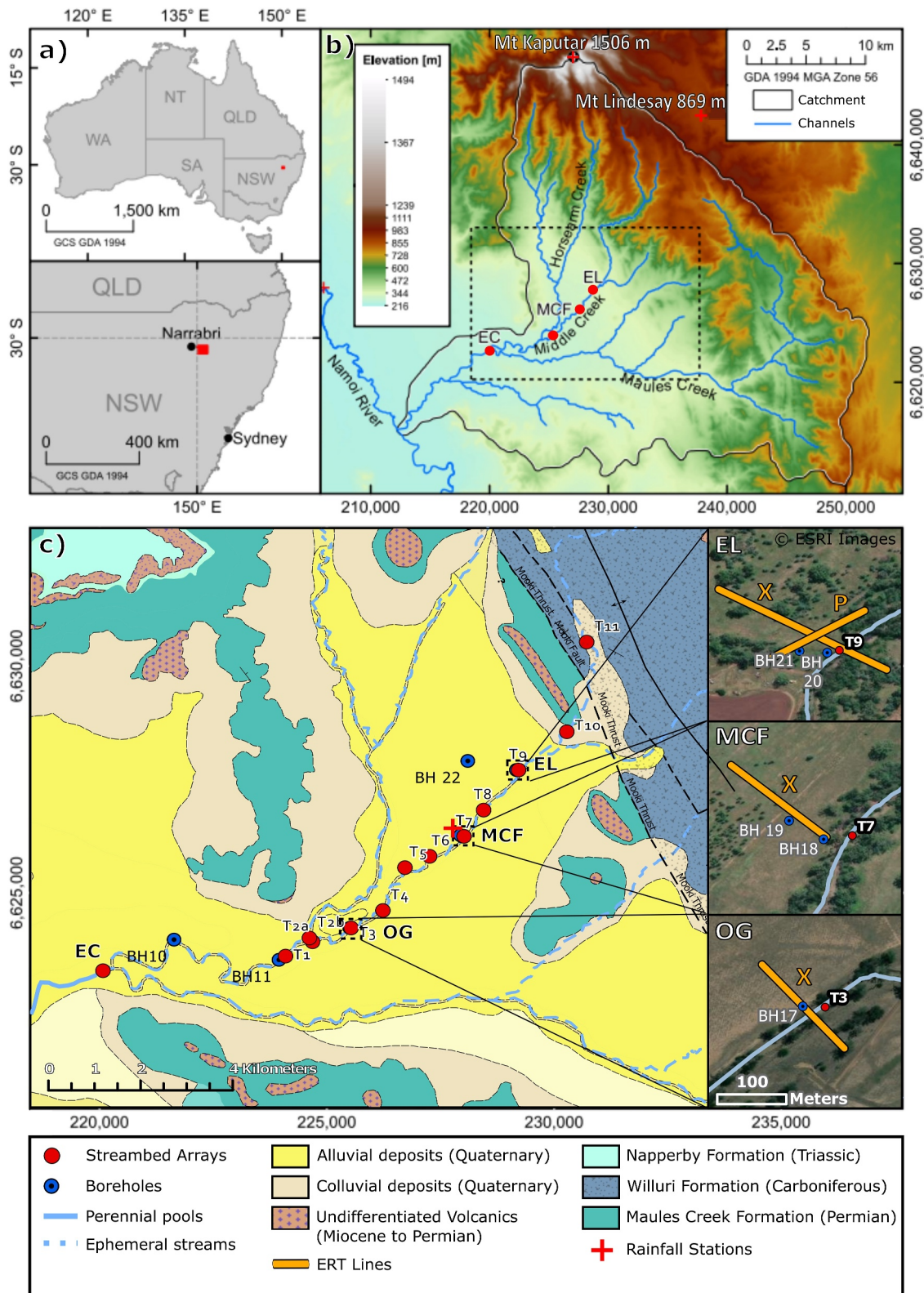


Figure 1.

106 km² of the upper catchment. Middle Creek joins another tributary, Horsearm Creek, about 4.3 km upstream from its confluence with Maules Creek near Elfin Crossing (Figure 1).

Rainfall is dominated by episodic frontal storms, the largest of which generally occurs in the summer months (December–February). Rainfall is also influenced by longer-term fluctuations in the El Niño Southern Oscillation Index (ENSO) and the Indian Ocean Dipole (IOD). Mean annual precipitation is 966 mm at the higher elevations of the Nandewar Range (Mt Kaputar) and decreases to 598 mm in the lower altitudes (Turrawan) of the catchment. Higher-than-average rainfalls occur in the positive phase (La Niña) and lower than average rainfalls in the negative phase (El Niño). Likewise higher rainfalls occur during negative IOD phases (Rutledge et al., 2023). Potential annual evapotranspiration (PET) is high and has been estimated as 1,200 mm in the Nandewar Range (Mt Lindesay), increasing to 1,800 mm in the lower altitudes (Turrawan) of the catchment (McCallum et al., 2013).

A geological map of the catchment is shown in Figure 1, and the geology of the catchment is summarized as follows. In the southern and western parts of the catchment the bedrock geology consists of Permian volcanic deposits of the Werrie Basalt formation. To the east, this formation is overlain by a sequence of Permian sedimentary deposits known as the Maules Creek formation, consisting of basal carbonaceous claystone, pelletoidal clay sandstone, minor coal, passing upwards into upward-fining cycles of sandstone, thinly bedded siltstone/sandstone, and coal. Toward the top of the formation, the stratigraphy becomes more conglomerate dominant. Excluding topographic highs and mafic intrusions of the Nandewar Volcanic Complex, this bedrock is generally overlain by Tertiary and Quaternary alluvial deposits consisting of clays, sands, and gravels. The Mooki Thrust zone runs approximately north-south through the Eastern part of the catchment and defines the mountain front, separating the Permian bedrock and alluvial cover from Carboniferous headwaters consisting of meta-sediments and volcanic deposits of the Willuri Formation.

Flow in Middle Creek is highly dependent on episodic frontal rainfall on the Nandewar Range that generates enough runoff in steep headwaters to deliver high energy flows across the mountain front. These flows have cut 10–15 m deep channels into Quaternary sediments which form the alluvial plain. These channels are filled with a heterogeneous assemblage of boulders, cobbles, sands, and gravels that are substantially reworked by each major flow event, typical of alluvium in episodic high energy streams (Shanfield et al., 2021). Middle Creek, Horsearm Creek and Maules Creek form a system of such intermittent channels. Except under periods of prolonged drought, flow at Elfin Crossing is perennial due to a zone of groundwater discharge (M. S. Andersen & Acworth, 2009; Rau et al., 2010) but ceases at some point between Elfin Crossing and the Namoi River because of losses to the underlying aquifer, partly due to groundwater abstraction for irrigation.

2.2. Monitoring of Rainfall, Groundwater, and Stream Stages/Flows

This Maules Creek catchment has been well instrumented since 2009 funded by the Australian Government's National Collaborative Research Infrastructure Strategy (NCRIS). Stream stage and groundwater heads were monitored at four locations within the study site (with abbreviations used in Figures 1–8 in brackets): (a) East Lynne (EL), (b) Middle Creek Farm (MCF), (c) Old Glenelg (OG), and (d) Elfin Crossing (EC) (Figure 1). East Lynne is located 2.5 km downstream of the foothills that form the headwaters and is the most upstream site. Middle Creek Farm, Old Glenelg and Elfin Crossing are located a further 4.5, 8, and 13 km downstream from the foothills. East Lynne, Middle Creek Farm, and Old Glenelg are located on Middle Creek, while Elfin Crossing is located at the confluence of Middle Creek and Maules Creek approx. 250 m downstream from the confluence of Middle Creek and Horsearm Creek and is the most downstream site in our work.

Multi-level boreholes (BH 17, BH 18, and BH 20 in Figure 1c) were installed adjacent to the creek, within tens of meters of the stream channel, at the four sites. Piezometric heads were monitored at 15-min intervals. Hyphenated numbers after borehole names (e.g., BH 20_2) correspond to screening depth, with 1–4 indicating shallow to

Figure 1. Map showing (a) Location of the Maules Creek catchment in relation to Australia and the state of New South Wales (b) Catchment digital elevation map (DEM) with locations Mt Kaputar and Mt Lindesay meteorological stations. DEM used courtesy of Geoscience Australia (c) Geological map (taken from Brown et al. (1992)) centered around Middle Creek, with streambed array installations and boreholes. EL = East Lynne; MCF = Middle Creek Farm, OG = Old Glenelg; EC = Elfin Crossing. Geological units in map are described in Section 2.1 (d) Geophysical survey lines with line names denoting location of survey. Suffix indicates whether line was parallel (P) or across (X) the stream (e.g., OG—X denotes line crosses the stream at Old Glenelg).

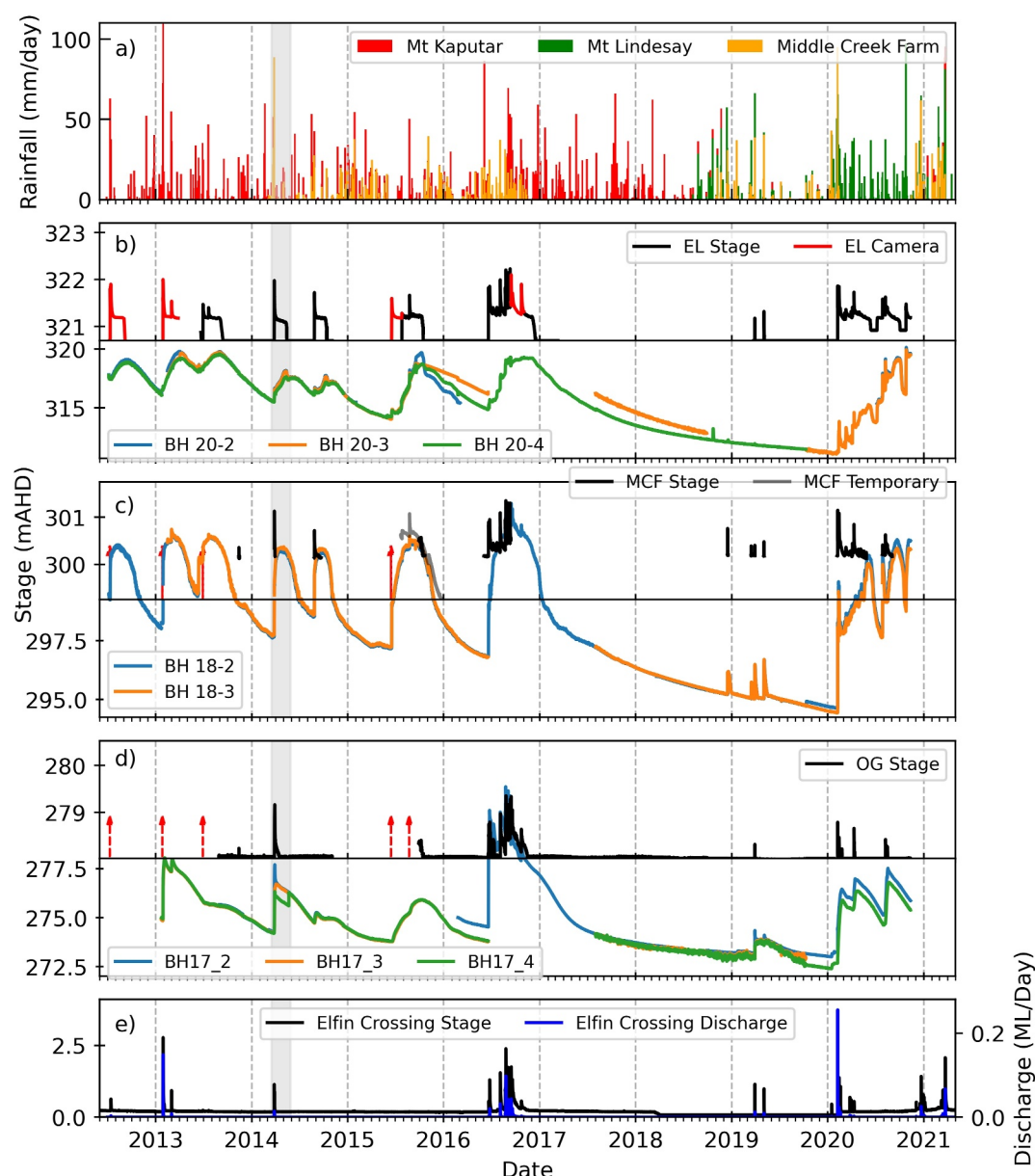


Figure 2. Time series compilation of composite (a) daily rainfall (b)–(d) stream stage hydrographs and groundwater heads and (e) Flow and stream stage at Elfin Crossing. Stream stage and groundwater recorded at the three study sites (East Lynne (b), Middle Creek Farm (c), and Old Glenelg (d)) were recorded at 15-min intervals but averaged over 1-hr periods to aid in smoothing data from barometric noise. The horizontal line in the middle of figures (b)–(d) denotes streambed, with y-axis scale changes taking place below and above the line. Red arrows denote streamflow events where there is missing data but responses can be inferred from the groundwater record. Shaded gray area denotes event captured in Figure 4. EL Camera denotes steam stage inferred from camera at East Lynne (see Section 2.2).

deep, respectively. Each multi-level borehole has a single 1-m screen, with the rest of the borehole cased out. The installation and setup of these boreholes are described by Cuthbert et al. (2016).

Stream stage was measured adjacent to boreholes at East Lynne, Middle Creek Farm and Old Glenelg using a Solinst Levellogger pressure transducer at 15-min intervals since June 2013. This logger was installed within a stilling well to mitigate the effects of surface water turbulence and flood wave action. A digital camera placed at East Lynne has been capturing a record of flows in the creek since June 2012 and was used to determine the timing and approximate magnitude of the flow events that were not captured by the logger (steamstage in red, Figure 2). Stream flow and stage at Elfin Crossing was taken from the permanent flow gauge station 49051 (Maules

Ck@Avoca East) established by the NSW Government (NSW Department of Primary Industries. <http://realtime.data.water.nsw.gov.au/water.stm>). Additional multilevel streambed arrays were installed at 11 different locations (T1–T11) along Middle Creek (Figure 1c) to capture the water level of flow events occurring in a 60-day period from 20th March to 18th May 2016. In addition, T3, T7, and T9 were installed at Old Glenelg, Middle Creek Farm and East Lynne respectively (see Figure 1c). Information on the details of this installation can be found in Rau et al. (2017).

Rainfall data was downloaded from the Australian Government Bureau of Meteorology (BoM) weather station directory for two locations: (a) Mt Kaputar National Park (BoM station #54151) and (b) Mt Lindesay Station (BoM station #54021, see Figure 1). Data from a full Campbell Scientific weather station installed next to BH19 at Middle Creek Farm was also used, representing rainfall on the alluvial plain. Most rainfall events were captured by the Mt Kaputar site and where rainfall data was missing, data from the Mt Lindesay and Middle Creek Farm were used to infill rainfall. For example, for the year 2020, the rainfall gauge at Mt Kaputar failed to record any rainfall, and data from Mt Lindesay and Middle Creek Farm form the composite record for that year. Double mass analysis between Mt Kaputar and Mt Lindesay, and Mt Kaputar and Middle Creek Farm indicate that rainfall is closely correlated ($r = 0.99$). This can be seen in Supporting Information S1 (Figures S1 and S2).

2.3. Subsurface Characterization

2.3.1. Electrical Resistivity Surveys

Electrical resistivity tomography (ERT) was selected to map and characterize superficial deposits for hydrological interpretation (Clifford & Binley, 2010; Cuthbert et al., 2009; Zarate et al., 2021). Four ERT surveys were conducted at East Lynne, Middle Creek Farm, and Old Glenelg sites in April 2014, the locations of which are shown inset in Figure 1d. Profile naming conventions correspond to location and orientation of line with respect to the creek. Profiles EL—X, MCF—X and OG—X correspond to transects taken perpendicular to (and across) Middle Creek at each of the study sites (apart from Elfin Crossing). Profile EL—P was taken perpendicular to profile EL—X and runs parallel to the creek at East Lynne.

An ABEM SAS4000 Terrameter with 2×32 takeout cables (2.5 m spacing) was used to perform the surveys, with profiles EL—P, MCF—X, and OG—X at 160 m length, and EL—X at 240 m length (see Figures 1d and 7). Note that at Middle Creek Farm, steep bank conditions prevented the profile from crossing the creek, and profile MCF—X therefore terminates just before the creek bank (location of stream channel is drawn on profile for reference). The Wenner electrode configuration was used to collect the data, and the steel electrode locations were prepared using a saline mud solution to reduce surface resistance. Topography was surveyed using leveling equipment.

The data was inverted using the RES2DINV (Geotomo Software) algorithm (Loke, 2006) and a limit of 4 iterations was set to avoid model over-fitting. An absolute error data constraint was used that minimizes the error between the observed and calculated apparent resistivity values. A robust model constraint, incorporating topographic variations, was selected over a least squared inversion constraint since it is known to better resolve sharp geological boundaries expected within the study area (Loke et al., 2003). In this case, it was important to delineate the boundaries between the superficial deposits. Inverted data are presented as geoelectric pseudo-sections (Edwards, 1977) and used in the interpretation of geoelectric layers and subsurface lithology.

2.3.2. Geophysical Well Logging

GEOVISTA borehole logging equipment (Geovista, United Kingdom) was used in the deeper boreholes to establish profiles of bulk electrical conductivity and gamma-ray activity. Data were recorded at 10-mm intervals using an induction sonde (EM53) and a gamma-ray activity sonde.

Borehole lithological data, ascertained from drillers logs, were used to aid in interpretation and correlation of well log data and corresponding lithology. While these logs often contained ambivalent lithological descriptions such as: “sand coarse some clay” or “clay sandy,” due to the mixed nature of drill cuttings, they can still help constrain the range of possible lithologies contained within the quaternary sediments. These logs were in turn used to correlate the values obtained from downhole geophysical logging to values found in existing literature on the resistivity of sediments.

2.3.3. Slug Testing

Slug tests were conducted by using a special device that seals the borehole and allows injecting compressed air to lower the water level in the piezometer by a few meters. After equilibration, the air was instantaneously released through a valve and the re-equilibration (i.e., relaxation) of the water level was recorded at high resolution. The test was repeated for each of the bores to ensure representative results. A total of 9 slug tests were performed on five boreholes at each of the three study sites. The analytical solution (following Hvorslev, 1951) was fitted to each of these data sets allowing averaging of the estimated sediment hydraulic conductivity values at the screened interval for each location.

3. Results

3.1. Hydrometric Monitoring

3.1.1. Rainfall

A composite daily rainfall record from Mt Kaputar, Mt Lindesay and Middle Creek Farm meteorological stations are shown for the period 1/7/2012–1/12/2021 (Figure 2). The largest rainfall event occurred on 2/2/2013 for both sites in the headwater catchment and was 149 and 150 mm/day for Mt Kaputar and Mt Lindesay, respectively. On the alluvial plain, the largest rainfall event occurred on 20/02/2020 for Middle Creek Farm and was 99 mm/day.

Rainfall varies spatially across the catchment due to the orographic effect of the mountains and increases with elevation. The highest values of 824 mm/year at Mt. Kaputar (1,506 m AHD, Australian Height Datum), and 679 mm/year at Mt Lindesay (869 m AHD) fall at the higher elevations (with both sites on the Nandewar Range), and the lowest values of 437 mm/year falling on the alluvial plain at Middle Creek Farm, (at 229 m AHD), only 19 km south Mt. Kaputar.

3.1.2. Streamflow Responses

Stream stage hydrographs at the four sites from the period 1/7/2012–1/12/2021 are shown in Figure 2. These data, taken at 15-min intervals, were averaged over 1-hr periods to aid in smoothing the data from barometric noise. These data show that streamflow across all sites (except for Elfin Crossing, which is perennial) is highly episodic and responds to periods of heavy rainfall concentrated over short durations in the headwaters (Figure 2). Not all these events lead to streamflow downstream however, and only events >66 mm/day generate enough streamflow to overcome channel transmission losses and appear at the furthest downstream site, Elfin Crossing. The highest recorded stage was in response to a large rain event occurring on the 25/08/2016. This event was not recorded by either rainfall gauge in the headwaters, however rainfall of 26.8 mm/day was recorded at Middle Creek Farm (on 24/08/2016).

Streamflow events at East Lynne exhibit a gradual flattening of the hydrograph after the streamflow peak followed by a period of stable water level where the hydrograph exhibits a long “shoulder” (Figure 3), and surface water is held within the channel at low flow rates. This behavior is observed after every streamflow event in the study period, apart from two streamflow events occurring during the 2019 drought, which had the smallest stage measurements on the record. A steady decline in water levels then follows this stable period, until streamflow finally ceases.

All streamflow events are shown in Figure 3, with each event plotted from their respective streamflow peaks and subsequent recessions (or as long as there is data available). Note that in cases where multiple streamflow peaks occur in a short space of time, the peak of the last streamflow event is used on the plot (see Figure S3 in Supporting Information S1 for plot containing previous events). When comparing each event, the duration of the streamflow “shoulders” after streamflow peaks remain remarkably consistent after every flow event in the time period ranging from 44 ± 3 days. This is despite large variations in stage (0.6–1.2 m) and flow (327–25,523 ML/Day, at Elfin Crossing), and there is no correlation (Pearson = -0.097) between the stream stage and duration of stable period at East Lynne (see Figure S4 in Supporting Information S1 for scatter plot).

When comparing the standard deviations (SD) to the mean values, the magnitude of stream stages show a much higher relative variance (SD = 28% of mean) than the variance in duration of streamflow (SD = 5.57% of mean). Furthermore, the SD in flows at Elfin Crossing are a much greater percentage of the mean (SD = 138% of mean),

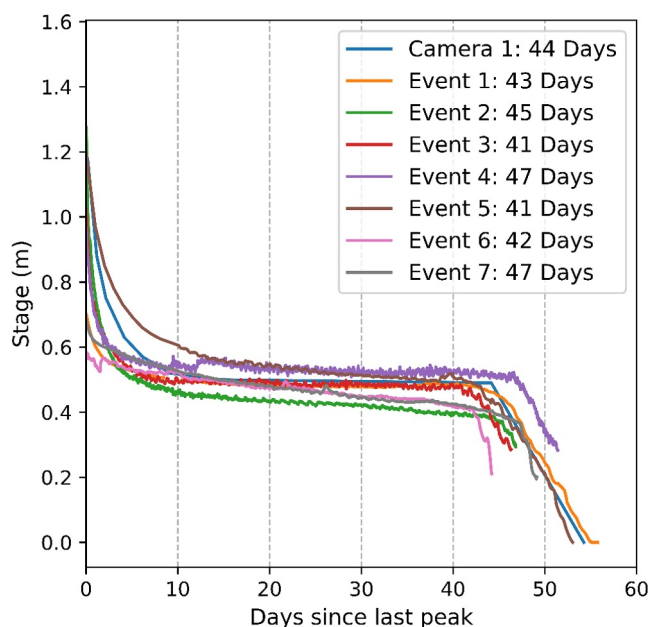


Figure 3. Streamflow hydrographs at East Lynne, plotted as days since the streamflow peak.

since the stage discharge relationship is not linear (see Figure S5 in Supporting Information S1 for rating curve at Elfin Crossing), albeit Elfin Crossing integrates a much larger catchment than Middle Creek.

Similar behavior cannot be confirmed at Middle Creek Farm however, as the logger was located at the end of a gravel bar. As such, the data captures only the peak stage of each flow event. A streambed logger installed in a lower elevation within the streambed captured stage for August–December 2015 (MCF temporary shown in gray in Figure 2), and shows water held in the channel for 35 days. In this instance, water held within the channel is due to groundwater levels rising above streambed elevation (see Section 3.1.3).

At Old Glenelg the streamflow hydrograph rapidly declines after the streamflow peak, exhibiting short periods of flow before becoming dry within 3–4 days of rainfall cessation, with no extended stable flow periods as seen at East Lynne. Elfin Crossing is generally perennial throughout the stage record due to groundwater discharge caused by a rise in the bedrock topography and a constriction of quaternary sediments at this site (M. S. Andersen & Acworth, 2009). It only became dry from March 2018 to January 2020, in response to a prolonged drought. The highest stream stage at Elfin Crossing was 3.2 m, in response to the rainfall in January 2020.

3.1.3. Groundwater Responses

Groundwater hydrographs are shown alongside stream stage at East Lynne, Middle Creek Farm and Old Glenelg for the period 1/7/2012–1/12/2021 in Figure 2. Heads varied between 0 and 8 m below ground level, with the thickness of the unsaturated zone generally increasing upstream. The groundwater responses are characterized by episodic rises that coincide with streamflow events along Middle Creek. Note that pressure or loading responses also occur at times of surface flows, as indicated by sudden increases in head in the groundwater hydrographs that correspond with onset of stream stage increases at the four sites. This is consistent with the variable lithology encountered during drilling, and the variability in formation hydraulic conductivity implied by slug testing, as described by Cuthbert et al. (2016) for a smaller number of events.

In general, following a flow event there is an increase in vertical hydraulic gradients between piezometers at each borehole, followed by a more gradual re-equilibration of heads. These can be interpreted as being due to vertical, transverse, and longitudinal propagation of the pressure increase induced by streamflow losses to the underlying alluvium working over different characteristic timescales (Cuthbert et al., 2016). Vertical downward hydraulic gradients are initially induced near the creek which then dissipate on the time scale of days to weeks (e.g.,

compare BH17_2 and BH17_4 in Figure 2). Longitudinal, down-catchment, gradients are apparent throughout the whole monitoring period suggesting they persist over longer time scales of years. These have an average horizontal gradient of 0.008 and indicate a general westward flow toward the Namoi River.

However, these groundwater responses vary at each study site. Heads in BH 20 (East Lynne) increase slowly in response to streamflow, peaking only when streamflow ceases at the site 44 ± 3 days after the streamflow peak. In BH18 (Middle Creek Farm), heads respond more rapidly to flow events and peak within 2–3 days of the streamflow peak. These heads plateau and remain at the same head for a further 32 ± 2 days. Data from a temporary streambed logger installed at Middle Creek Farm for the period August–December 2015 show that water is held within the channel when groundwater levels remain above the streambed elevation. As such, surface water may be held within the stream for much longer than is seen in the stream hydrograph data at Middle Creek Farm, which only captures the peak of such flow events due its location on an elevated gravel bar in the streambed.

At BH17 (Old Glenelg), heads also rapidly increase in response to streamflow and peak within days of a flow event but fall much more quickly when streamflow ceases at the site 3–4 days after the streamflow peak. These large fluctuations in heads interrupt long-term groundwater recessionary trends of various lengths, the steepness of which decreases downstream. During periods of prolonged no-flow from January 2017 to January 2020, heads fell to 9 m below the surface adjacent to the streambed at East Lynne, 6 m below at Middle Creek Farm, and 5 m below at Old Glenelg.

3.1.4. Spatially Detailed Hydrological Responses to a Single Runoff Event (20th March–18th May 2014)

To further examine the dynamics of streamflow variations along Middle Creek, data from 8 pressure loggers that recorded stream stage from 20th March to 18th May 2014 were plotted alongside nearby boreholes and are shown in Figure 4. This data is also presented in Rau et al. (2017), and illustrates the variation in stream hydrograph dynamics for one streamflow event at high spatial resolution but re-interpreted in light of additional data presented here. Site T9 is located at East Lynne, T7 at Middle Creek Farm and T3 and Old Glenelg (see Figure 1c for locations of pressure loggers). This flow event is also captured in time series compilation in Figure 2 and is shown in the shaded area in gray.

Streamflow hydrographs in this compilation behave differently for each array along the flow path (Figure 4). Arrays T11 and T10 exhibit the similar characteristics to long term streamflow behavior seen at the East Lynne (T9) site (Figure 2). These upstream arrays (T11–T9) all show long hydrograph “shoulders” (representing periods of stable water level) that increase downstream, from 22 days in T11 to 44 days at T9. Based on the long-term groundwater responses at T7 (Figure 2), it is likely that streamflow exists at a longer duration than indicated by the logger (which is situated on a bank with higher elevation than the bottom of the streambed) and water exists within the streambed at T7 for at least as long as T10. Downstream of T7, hydrograph shoulder lengths reduce substantially and exhibit rapid rises in groundwater levels 2 days after the streamflow peak, before quickly receding. Looking at the long-term trends (Figure 2), these dynamics appear to be consistent in their shape and size during each runoff event, regardless of the size of rainfall event and subsequent runoff intensity (Figure 3).

3.2. Subsurface Characterization

3.2.1. Geophysical Well Logging

A total of 6 downhole geophysical logs covering all three study sites (a list of boreholes and associated lithological logs where the downhole geophysical logs were performed can be found in Table 1). Integrating the results of the downhole geophysical logs with borehole log lithologies (as described in Section 2.3.2) identify four lithological groups in the system using existing literature (Rubin & Hubbard, 2006) for typical resistivity or electrical conductivity ranges of sediments:

- Sands and Gravels ($>200 \Omega \text{ m}$ or $<5 \text{ mS/m}$)
- Interbedded Sands and Clays ($200\text{--}50 \Omega \text{ m}$ or 5 to 20 mS/m)
- Clay dominated ($50\text{--}20 \Omega \text{ m}$ or 20 to 50 mS/m)
- Sedimentary rocks ($<20 \Omega \text{ m}$ or $>50 \text{ mS/m}$).

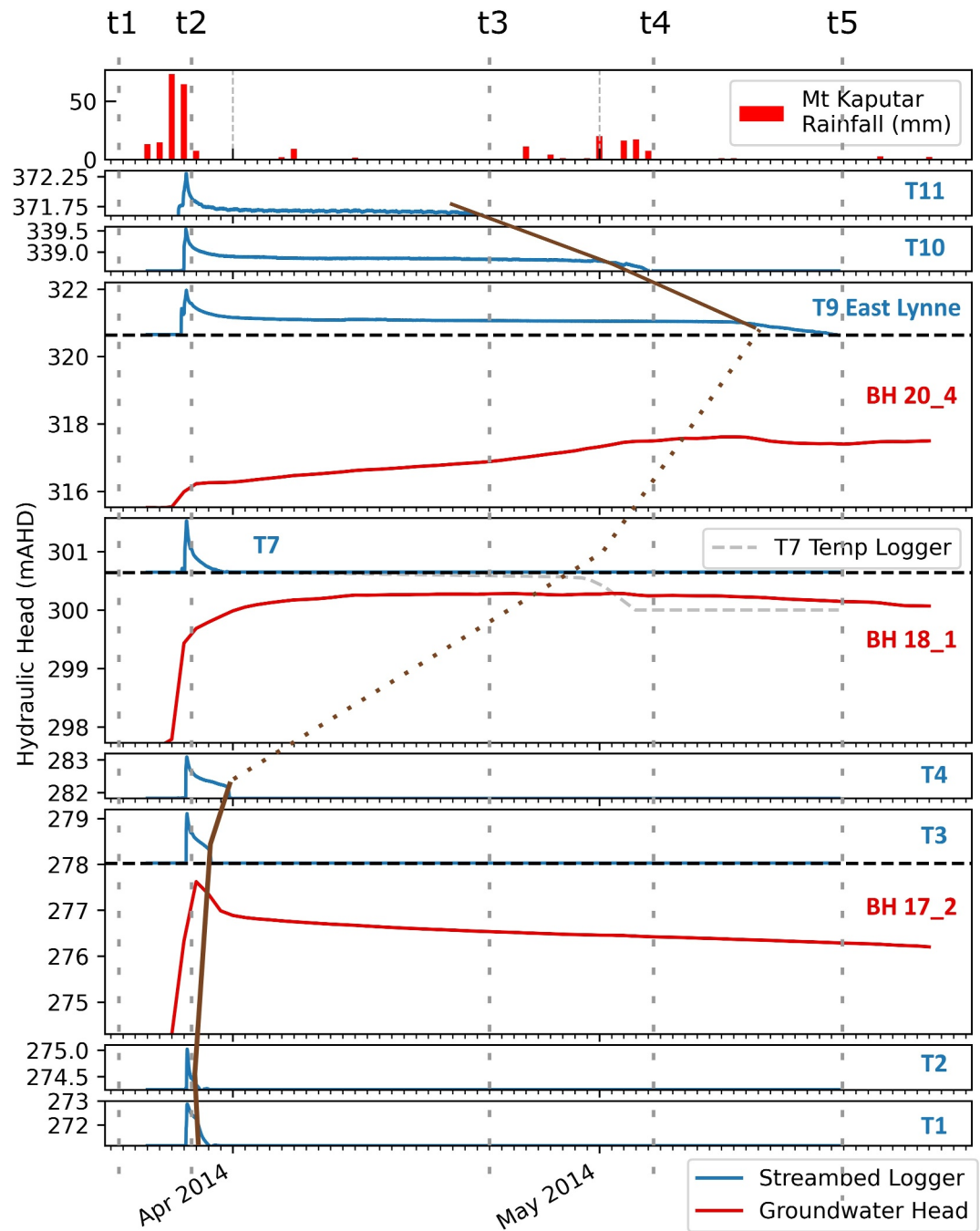


Figure 4. Daily rainfall recorded at Mount Kaputar and hydraulic heads recorded by temporary streambed arrays installed along Middle Creek, including nearby groundwater heads. Dotted vertical lines indicate time periods described in Section 3.3. Brown lines highlight increasing streamflow “shoulders” from T11 to T9 and decreasing shoulders from T9 to T1. Note that as the streambed logger at T7 was situated on a bank, it does not capture full extent of streamflow and this shoulder is inferred by the dashed line. The data is reinterpreted from Rau et al. (2017).

These interpreted lithological groups and electrical conductivity ranges are shown superimposed onto the geophysical logs at each study site on Figures 5 and 6. Note that more detailed classification is made when describing the lithology of the Permian sedimentary rocks, where the exact interpretation from the drillers logs is used for each borehole (e.g., Sandstone or Shale). It is also worth noting that the high electrical conductivity for

Table 1
Hydraulic Conductivity Values of Boreholes at Various Depths, Obtained via Slug Testing

BH	Hydraulic conductivity (m/d)	Depth to base of 1 m screen (m)	Interpreted lithology
17_2	Test failure	13.5	Interbedded Sands and Clays
17_4	0.34	36.5	Permian Sandstone
18_2	0.47	12	Interbedded Sands and Clays
18_4	0.08	24	Permian Bedrock (lithology unknown)
19_1	0.02	11.5	Clay Dominated
19_2	0.04	23	Clay Dominated
20_2	0.02	12	Clay Dominated
20_4	Test failure	41	Permian Shale
21_2	0.003	13.5	Clay Dominated

Note. Boreholes are only screened for the 1 m at the depth stated, with the rest of the borehole cased out. Interpreted lithology from Section 3.2.1 also added.

the Permian sedimentary rocks is likely to be a function of high electrical conductivity pore fluids (groundwater), rather than just rock properties. A more than 50 m deep exploration bore was sampled in 2010 and returned a fluid electrical conductivity of 2,260 mS/m. Barrett (2012) have reported that fractured rock aquifers of the region generally have salinities, expressed as electrical conductivity (EC), in the range from 1,000 to 7,000 $\mu\text{S}/\text{cm}$.

In the Quaternary sediments, the gamma-logs have problems distinguishing between clay, sand, and gravel lithologies noted in the driller's logs. This effect was also observed in M. S. Andersen and Acworth (2009), who hypothesized that the Quaternary sands and gravels of the Maules Creek catchment, derived from the volcanic Mt Kaputar complex, are only weakly weathered and contain a very high potassium content. As such, the total potassium content in the clay layers and the coarser alluvium would be very similar and therefore indistinguishable in the gamma logs. In this geological setting, the gamma-log is a poor tool for distinguishing between the lithologies within the Quaternary alluvium.

Although the gamma logs do not exhibit any differences between the clay, sand, and gravel changes noted in the core logs, they do exhibit notable decreases at 20 and 23 m in BH17 and BH20, respectively, coincident with large increases in bulk EC and a change from Quaternary sediments to Permian sedimentary rocks in the driller's logs. This decrease in gamma activity is likely representative of a change in lithology from potassium-rich Quaternary deposits to more potassium-deprived Permian (Maules Creek formation) sediments beneath.

In contrast, the bulk EC shows clear differences between the boreholes in the uppermost Quaternary sediments. These differences are highlighted in Figure 6, where a smaller scale (0–80 mS/m) is used to distinguish lithologies at lower bulk EC typical of unconsolidated deposits. In the uppermost 12 m, the sediments at BH17 consist of low EC sands & gravels. These transition to sands with interbedded clays and finally clays before reaching the much higher EC Permian sedimentary rocks (primarily sandstone, as noted in the drillers logs), which reaches ECs of up to 400 mS/m (see Figure 5). As mentioned above, these high bulk ECs in the Permian are likely due to the brackish nature of the deeper groundwater in the catchment.

In BH18 and BH20, the sediments consist of sands and clays in the uppermost 3 m. Below this depth, the lithology is dominated by higher EC clays with possible layers of lower EC interbedded sands (at 11 m in BH18, and 17 m in BH20). In BH20 there is again a sharp increase in bulk EC (coincident with gamma decrease), signaling a transition into Permian sedimentary rocks (identified as shales in the drillers logs). Note that at BH18, both drillers' logs and geophysical well logs only extend to a depth of 23 m, and any interface to the Permian was not captured at this site.

3.2.2. Electrical Resistivity Imaging

ERT profiles taken at each of the study sites, locations of which are shown in insert in Figure 1, are shown in Figure 7. Boreholes with interpreted lithology based on combined data from geophysical well logging and drill

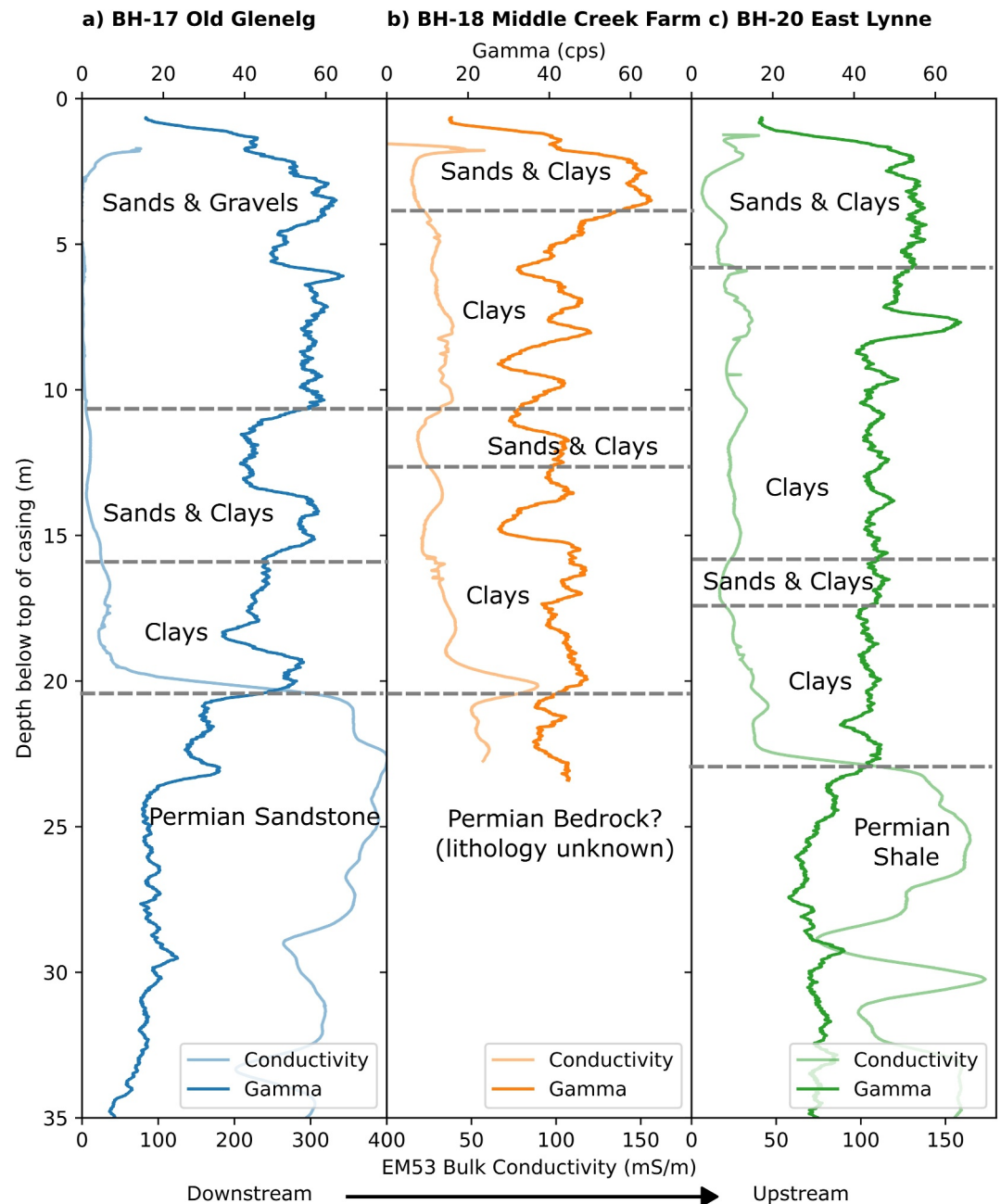


Figure 5. Geophysical logs for boreholes at each of the three study sites. Lithological data taken from drill cuttings were used to aid in lithological interpretations of the data and these interpretations are superimposed. Note that BH18 was not drilled to the depth of the Permian sedimentary rock and as such the interface and lithology here are unknown.

cuttings (see Section 3.2.1) are superimposed. These were used to aid in interpretations of lithological layers described below.

3.2.2.1. East Lynne

The profiles taken at East Lynne (EL-P & EL-X) show a 3–5 m thick upper zone with resistivity ranging from 70 to 300 Ω m interpreted as sands & clays. In profile EL-X, the alluvium surrounding the creek bed is apparent, exhibiting very high resistivities >300 Ω m. Pockets of this high resistivity alluvium appear to be present on the middle and left side of profile EL-X and are interpreted as former channels. Below this zone, the profile becomes

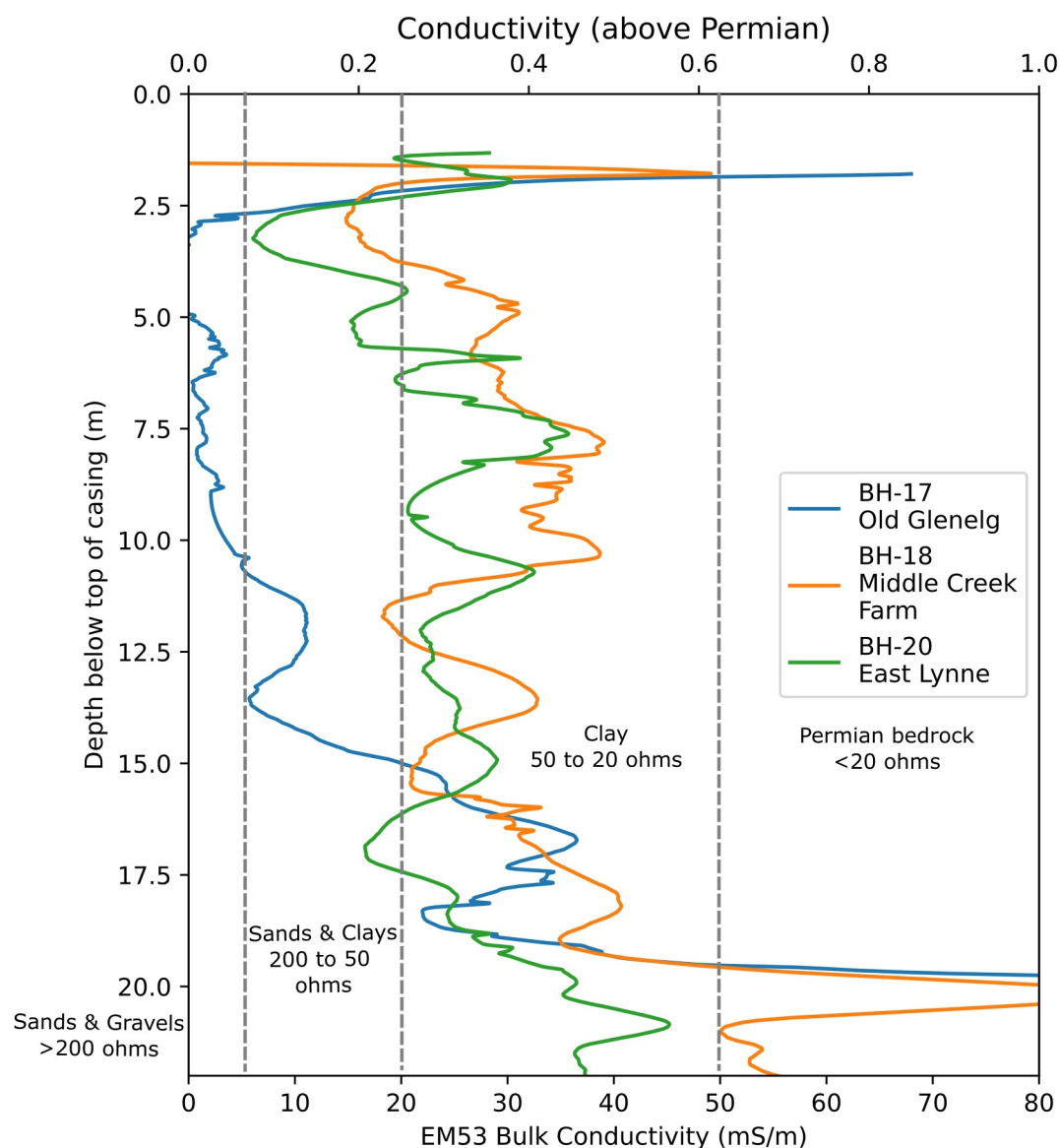


Figure 6. EM53 Bulk electrical conductivity logs with smaller scale (0–80 mS/m) to highlight variations in electrical conductivity of quaternary sediments. Lithological interpretations with the aid of drill cuttings are superimposed alongside resistivity ranges.

less resistive with depth, with resistivities falling between 10 and 50 Ω m, and the lithology is interpreted to be clay dominated. At the very bottom of the profiles, the Permian shale begins to have an influence, with resistivity dropping below 10 Ω m.

3.2.2.2. Middle Creek Farm

The line taken perpendicular to the creek at Middle Creek Farm (MCF-X) exhibits a similar resistivity profile to East Lynne (profiles EL-P & EL-X) with a thin zone (0.5–1 m thick) of low resistivity (15–30 Ω m) material at the top of the profile. Below this, there exists a layer (5–8 m thick) of higher resistivity (50–100 Ω m) material, interpreted as sands and clays. Like profile EL-X, a prominent pocket of high resistivity (>300 Ω m) material is seen on the left side of the profile, 1 m below the surface, indicating the presence of a former channel. At 10 m, the lithology becomes less resistive and is interpreted to be clay dominated. At 20 m depth, the resistivity again drops below 10 Ω m as the low resistivity Permian affects the profile. Note that the presence of Permian here is an interpretation as drillers and geophysical well logs at this location do not extend this deep.

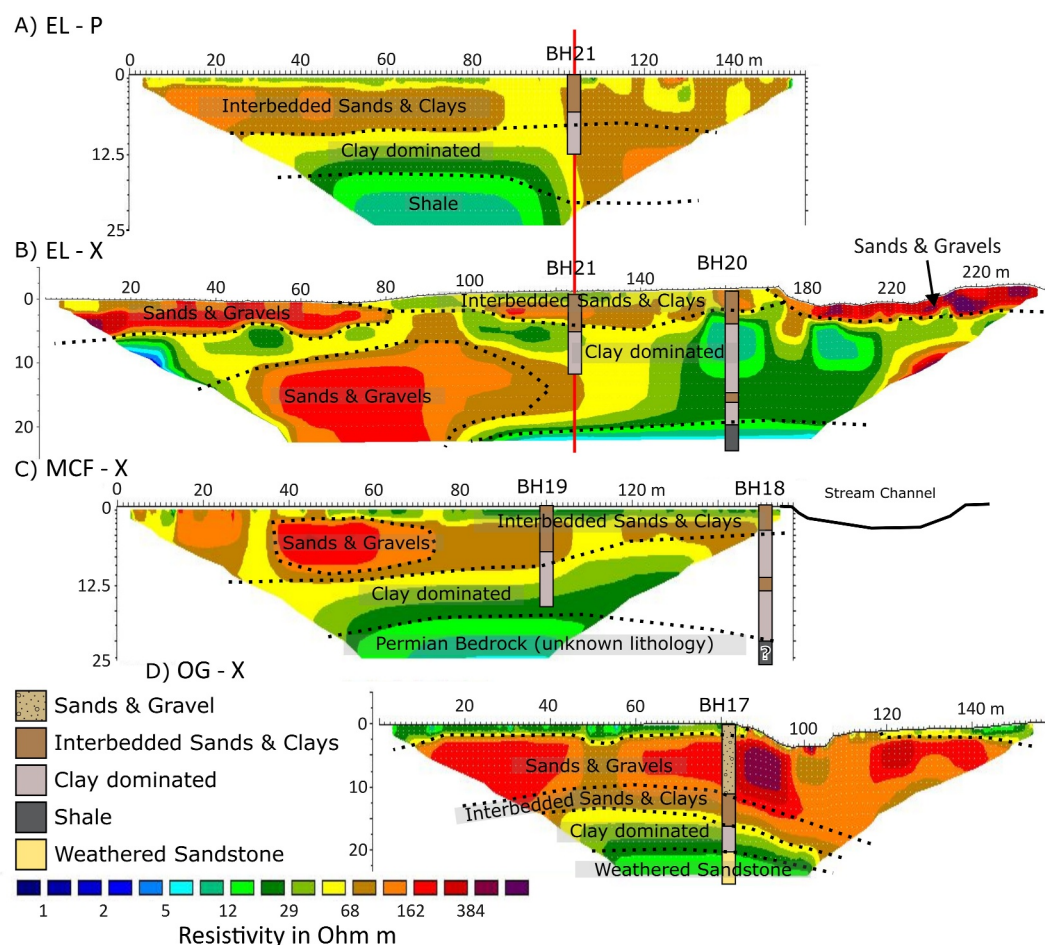


Figure 7. Electrical Resistivity Tomography (ERT) of transects taken at each study site. Locations of boreholes in relation to the lines are shown and lithological interpretations from Section 3.2.1 are superimposed onto the boreholes. Panels are offset to conceptually represent their location with respect to the channel in space. Intersection point between lines EL -P and EL-X at East Lynne is shown in red.

3.2.2.3. Old Glenelg

In profile OG-X, a thin layer of low resistivity topsoil, like that in profile MCF-X, can be seen in as a continuous layer 1–2 m thick extending across the profile. This layer is interrupted at the stream channel by the presence of higher resistivity (200–300 Ω m) streambed alluvium. However, it is difficult to distinguish the geometry of this alluvial material, as the underlying geology consists of similar high resistivity (150–350 Ω m) materials, interpreted as sands and gravels. This layer of sands and gravels extends from 1 to 11 m below the surface, before transitioning to a zone of lower resistivity (10–50 Ω m) material interpreted as clay dominated and finally Permian sandstone (10 Ω m) at a depth of 23 m. Pockets of higher resistivity (>300 Ω m), as seen in profiles EL-X and MCF-X, can also be seen in the sands and gravels on the left- and right-hand sides of profile OG-X. These former channels exist at all three study sites, and satellite imagery confirms the continuity of the channels at the ground surface. The continuity and geometry of the former channels at depth is unknown.

3.2.3. Aquifer Properties

The results of hydraulic (slug) testing are shown in Table 1, as well as the lithology at each borehole interpreted in Section 3.2.2. Due to low hydraulic conductivity of materials surrounding the well screen, the test at BH20_4 failed. The hydraulic test in BH17-2 failed for unknown reasons.

The results show low hydraulic conductivity sediments of 0.021 m/day, interpreted as clay dominated, at depths of 12 m at BH20_2, 2 m away from the stream, at East Lynne. This hydraulic conductivity decreases to 0.003 m/

day at BH21_2, which is a further 37 m away. In the interpretation of downhole geophysical logs, sediments in boreholes at these depths were classified as clay dominated.

Sediments with similar hydraulic conductivities (0.017 m/day) as BH_20 are present at the same depth (11.5 m) at BH19_1 at Middle Creek Farm, situated 50 m away from the stream. Hydraulic conductivity increases closer to the stream, as observed at BH18, which is situated 10 m away from the stream, with values increasing from 0.017 to 0.470 m/day at the same depth. These changes in hydraulic conductivity correspond to a change in lithology from clays to interbedded sands and clays. In BH18 at Middle Creek Farm, hydraulic conductivity decreases with depth, from 0.470 m/day at 12–0.075 m/day at 24 m. However, since driller's logs did not extend to this depth, the lithology is unknown and could be interpreted as Permian sediments (see Section 3.2.1). At greater depths (41 m) the Permian sandstones at Old Glenelg exhibit hydraulic conductivities of 0.340 m/day and are at the same order of magnitude as the sands and clays recorded at 12 m at BH18_2.

3.3. An Alluvial Storage Model for Controlling Water Balance Partitioning in Middle Creek

The results in Figures 2–4 illustrate the complex surface water-groundwater dynamics and water balance partitioning at Middle Creek. Based on these data, a hydrogeological conceptual model of the Middle Creek stream system was developed (Figure 8) that seeks to explain the complex surface water - groundwater dynamics by way of variations in superficial geology at each site. Using time periods defined in Figure 4 (t1–t5), we propose that the superficial geology surrounding Middle Creek controls water balance partitioning over time as follows:

t1: Streamflow is non-existent in the creek and the groundwater system is in a long-term longitudinal recession. Large frontal storms generate orographic rainfall that quickly causes infiltration excess overland flow and large amounts of runoff are discharged across the mountain front. This is consistent with streamflow generation in dryland ephemeral streams, where, due to orographic effects, streamflow often begins in the mountain headwaters and upstream reaches of a catchment, and propagates downstream (Bull & Kirkby, 2002; Godsey & Kirchner, 2014; Shanafield et al., 2021).

t2: Runoff coalesces into ephemeral streams and the streamflow flood wave propagates downstream. As this runoff infiltrates the streambed, a perched groundwater mound saturates the streambed from the bottom upwards (Dahan et al., 2008; Moulahoum, 2018; Wekesa et al., 2020) quickly filling the available “alluvial storage” in the highly permeable alluvium (Telvari et al., 1998). The streamflow peaks in 1–2 days as the flood peak passes. Upstream of Middle Creek Farm (T11–T7), the high “permeability contrast” between alluvial material and surrounding low permeability (clay dominated) deposits slows the vertical infiltration of perched alluvial water. Groundwater mounding also occurs in the deeper aquifer beneath the alluvium, but its rise is slow due to the permeability contrast. Perched alluvial water is instead preferentially partitioned longitudinally downstream within the alluvium and to discharge as streamflow from T11 to T7, akin to bank storage. Rapid vertical infiltration occurs only where streamflow reaches higher permeability Quaternary sands and gravels downstream of Middle Creek Farm (T7) and toward Old Glenelg (T3). Here infiltrating streamflow quickly fills the unsaturated zone between the water table and the stream, and groundwater within the Quaternary deposits rises rapidly.

t3: Streamflow ceases at T11, but infiltrated water retained within the alluvium at T11 maintains subsurface longitudinal drainage downstream to T10 due to the high permeability contrast between the alluvium and the underlying geology. This subsurface longitudinal drainage keeps downstream alluvial storage full, and due to the slope of the channel, manifests as flow within the streambed from T10 to T7. Downstream of this site (T7–T1), higher permeability sands begin to dominate the sediments surrounding the alluvium, and vertical flow is no longer slowed by high permeability contrasts. Vertical infiltration into these sediments becomes greater than the incoming flow from stored alluvial water, causing the groundwater mound that has formed within the alluvium at these sites to dissipate more rapidly than upstream. As a result, the water table drops below the streambed more quickly, causing surface flow to cease at Old Glenelg.

t4: Despite a small storm that occurs on 04/05/2014, by t4, stable streamflow persists longer downstream from T11–T9, owing to cumulated increased volume of alluvial store (and therefore alluvial water flowing longitudinally) upstream of each site. Eventually streamflow only exists at East Lynne (T9), and streamflow duration ends at 44 ± 3 days. In this period of stable streamflow, some water in the perched saturated alluvium continues to slowly infiltrate vertically and recharge the aquifer below, causing the deeper groundwater mound to grow.

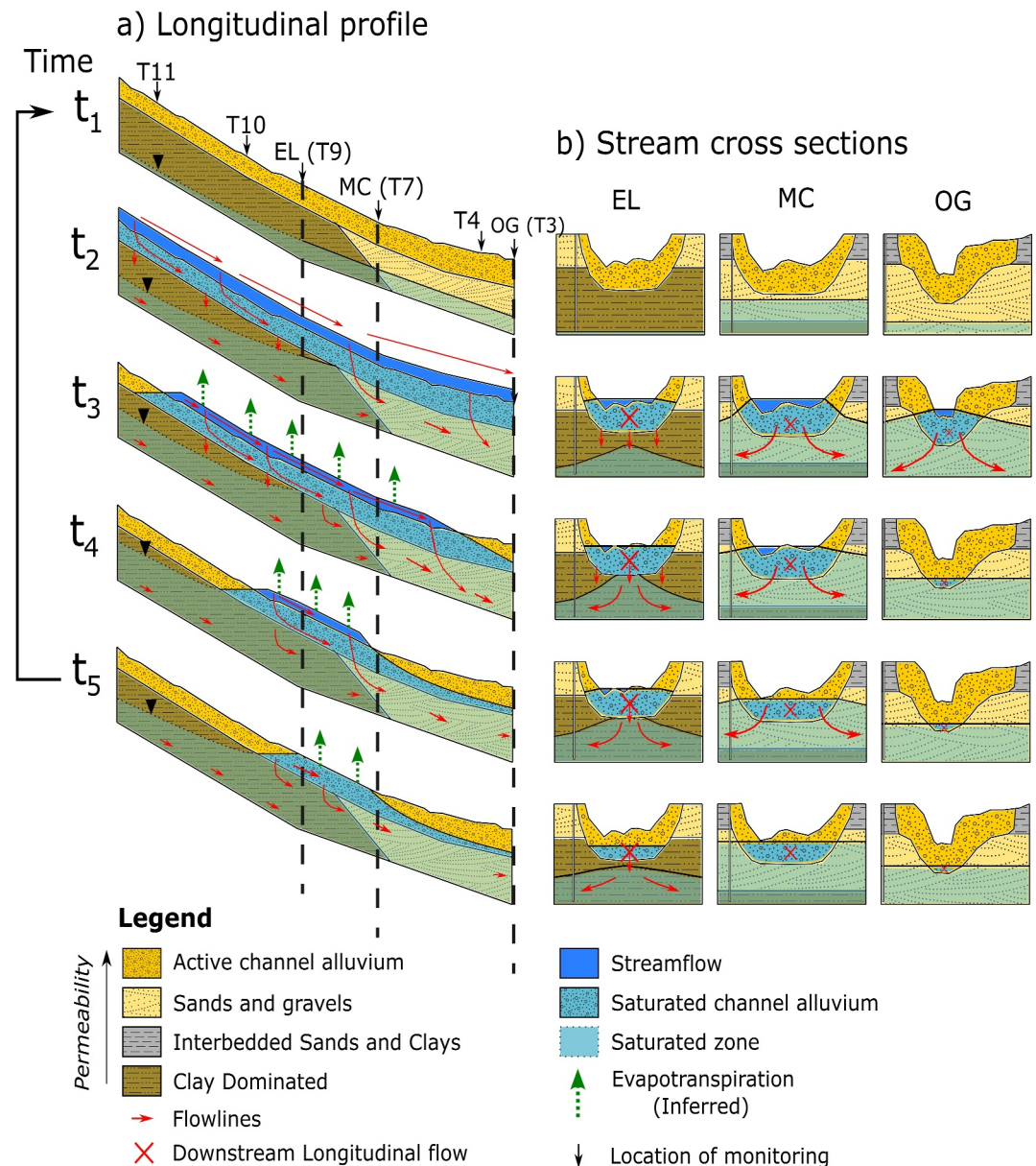


Figure 8. Conceptual model of how superficial geological structure controls water balance partitioning and streamflow generation in Middle Creek as representative of a typical IRES system. Dashed vertical lines correspond to stream cross sections, which were inferred from geophysics (see Figure 7). Size of downstream longitudinal flow symbol denotes the magnitude of flux. Since there are no direct measurements of evapotranspiration at the study site, it is instead noted as inferred in this model (denoted by the dashed symbology).

t_5 : After 45 days, alluvial water storage upstream from T_9 has been completely drained longitudinally and flow within the stream ceases, and the stream becomes dry once again. Eventually, the groundwater mound fully redistributes, so that only long-term longitudinal groundwater recession is occurring again.

4. Discussion

There is a growing body of literature using near-surface geophysics to understand IRES dynamics (Callegary et al., 2007; Lorentz et al., 2020; Shanafield et al., 2020; Zarate et al., 2021). However, these often lack crucial information such as hydrometric data or spatial resolution to capture the complex spatial variation in streamflow and groundwater dynamics associated with water balance partitioning in IRES. Furthermore, while multi-year

observations of groundwater dynamics in IRES exist, these have only been reported for few sites worldwide (e.g., Carling et al., 2012; Dahan et al., 2008; Fuchs et al., 2019; Pool, 2005; Zipper et al., 2022). Consequently, we consider our observations to consist of an unusually rich data set in both space and time, allowing an unprecedented insight into both stream flow dynamics and its control by the underlying geological structure.

Our conceptual model outlines two dominant controls on water balance partitioning in intermittent rivers and ephemeral streams:

- The permeability contrast between recent streambed alluvium and underlying (and surrounding) geology, and
- The volume of recent alluvium, which we call the “alluvial store” at, and upstream, of a site. In areas of high permeability contrast (i.e., high permeability recent alluvium and lower permeability in the surrounding geology), restricted vertical infiltration into low hydraulic conductivity materials allows for perched water and preferential longitudinal flow within recent alluvium, keeping alluvial stores downstream “topped up” even when streamflow upstream has ceased. In areas of low contrast (i.e., high permeability recent alluvium surrounded by similar high permeability geology), perched water is unable to form, and instead streamflow is partitioned vertically to a greater extent, increasing soil moisture in the unsaturated zone, and recharging the water table within the high hydraulic conductivity surrounding lithology.

The volume of recent alluvium at a particular site, and upstream of it, will also vary depending on stream order and position within the catchment (Jaeger et al., 2017). In channels located upstream, which drain a smaller area of catchment, there is not only a smaller alluvial store, but also less contributions in longitudinal flow due to a smaller volume of alluvial store upstream. Downstream reaches, which drain a greater extent of the catchment, also receive a greater volume of potential alluvial water from upstream reaches.

The dominant controls outlined in our conceptual model are widely transferable to other dryland catchments. High permeability contrasts between permeable alluvium and underlying low hydraulic conductivity geology seen at East Lynne and Middle Creek Farm appear to be common features in dryland ephemeral streams worldwide (Acworth et al., 2020; Brunner et al., 2011; Goodrich et al., 2004; Lorentz et al., 2020; Rassam et al., 2006; Séguis et al., 2011; Shanafield et al., 2021; Villeneuve et al., 2015), and have been shown to control streamflow generation in dryland IRES (Bourke et al., 2021). At Old Glenelg, where there is a low permeability contrast, stream stage and groundwater responses are consistent with the dynamics of ephemeral streams where large unsaturated zones exist, and rapid vertical infiltration and streamflow cessation occurs (Brunner et al., 2011; Partington et al., 2023; Quichimbo et al., 2020; Shanafield & Cook, 2014).

The partitioning of alluvial water into streamflow due to this contrast can be seen in the ephemeral sand rivers of southern Africa, where streamflow occurs via saturation excess only after the streambed “alluvial store” has been filled (Dahlin & Owen, 1998; Hughes, 2008; Partington et al., 2023). This observation is consistent with the work of Lange et al. (1998), who found via artificial tracers that infiltrated streamflow within the alluvial store reappears on the surface downstream. In the crystalline basements of western Africa, Séguis et al. (2011) also found that alluvial stores of seasonal perched groundwaters are the major contributor to streamflow.

Perched alluvial water provides a valuable supply of accessible water for local people that is commonly exploited either by shallow pits dug in the sand or by well-points, infiltration galleries or collector wells in the river bank (Hussey, 1997). Furthermore, this perched alluvial store has been shown to be enhanced by the construction of sand dams in southern Africa (Love et al., 2010).

Although there are no direct measurements of evapotranspiration at the study site, in the period where extended durations of perched water exist within the alluvial store, evapotranspiration from riparian vegetation will be high since it has access to a readily available, shallow store of water (Scott et al., 2008). The alluvial store also allows more abundant and functionally diverse vegetation to develop in riparian areas (Shaw & Cooper, 2008). Perched water within this alluvial store is often entirely consumed by trees and other vegetation and in some IRES evapotranspiration from this perched alluvial store can account for up to 100% of streamflow, and regional groundwater recharge is negligible (Bauer et al., 2006; Villeneuve et al., 2015). In Australia, water within perched aquifer systems plays a crucial role in maintaining *Eucalyptus camaldulensis* trees (Cook et al., 2008).

At East Lynne, the stream stage hydrograph exhibits the longest period of flow, due to a combination of high permeability contrast and the contribution from alluvial stores of water upstream via longitudinal flow. Thus, at Middle Creek, the combination of these two controls creates a “goldilocks zone” of stream flow duration and

perched water presence within the alluvium, maximizing both riparian water availability within the alluvium, and the potential for groundwater recharge due to the maximal persistence of this perched water. The two dominant controls from our conceptual model likely exist as a continuum in dryland catchments globally where these two controls interact and align, and we hypothesize that the combination of these two controls, the permeability contrast and size of alluvial store upstream, may create goldilocks zones where various components of the water balance (e.g., evapotranspiration, groundwater recharge) are likely maximized.

These processes are not exclusive to dryland IRES either. In the humid soils of North Carolina, Zimmer and McGlynn (2017) found that near surface stores of perched water were the main contributors persistent streamflow in an intermittent stream. In the headwaters of the humid Konza Prairie in Kansas, Swenson et al. (2024) found near surface sources of water sustained flows in a non-perennial network of streams during periods with variable hydrological conditions, such as the summer dry down season. Along an intermittent reach of the Arkansas River, Koehn et al. (2020) found that spatial changes in superficial geology highlighted the role of riverbed heterogeneity in controlling localized recharge to the underlying Ogallala Aquifer. As such, our model may be more broadly transferable to represent humid IRES in headwater catchments, or those sensitive to seasonal fluctuations.

Our findings, while bearing resemblance to previous research conducted at sites experiencing episodic groundwater recharge triggered by high-intensity rainfall events (e.g., Jasechko & Taylor, 2015; Lange, 2005; Owor et al., 2009; Seddon et al., 2021; Taylor, Scanlon, et al., 2013; Taylor, Todd, et al., 2013) reveal distinctive temporal dynamics in streamflow characteristics and groundwater responses in our study area, as illustrated in Figure 2. These trends suggest that groundwater recharge is controlled by streamflow duration, a parameter seemingly unaffected by the magnitude of rainfall and ensuing runoff events, as depicted in Figure 3.

This intriguing observation prompts further exploration. We have determined that geological factors govern streamflow duration, stabilizing it at approximately 44 ± 3 days in our system. Interestingly, the most significant recharge events within the catchment materialize when multiple streamflow events overlap, extending the stream's flow period well beyond the typical 47-day limit. For example, an event that began on 18/06/2018 led to 184 days of uninterrupted streamflow in the creek, 3.9 times the typical 47-day limit for singular events.

While regional climate projections indicate a consistent mean annual rainfall, albeit with a shift towards more intense precipitation events (Taylor, Scanlon, et al., 2013; Taylor, Todd, et al., 2013) our study postulates a novel perspective. We suggest that it is not the intensity of rainfall and the resulting flow magnitude that primarily control groundwater recharge in our locality. Instead, we propose that the frequency of flow events exerts more influence.

This hypothesis warrants comprehensive examination in future studies, as it carries substantial implications for understanding groundwater recharge dynamics and ecosystem functionality under evolving climatic and hydrological conditions. Consequently, it underscores the critical need to incorporate geological considerations into hydrological stream classifications, a facet that has hitherto been overlooked.

5. Conclusion

We examined variations in superficial geology and relationships between rainfall, streamflow, and groundwater in an intermittent stream system in semi-arid Australia. We consider this data set to be unusually rich in both time and space. Spatially detailed responses to a single runoff event reveal that periods of highly stable stream-stage (following streamflow peaks) increase in the downstream direction to a maximum, before abruptly reducing further downstream. Long-term hydrometric monitoring confirms that streamflow lasts 44 ± 3 days after each streamflow peak and is independent of the size of the preceding streamflow peak.

A comprehensive assessment of the superficial geology around the stream was conducted using a blend of downhole geophysical logging, near-surface electrical resistivity imaging, and slug testing. This investigation unveiled a distinctive hydrogeological pattern in the Quaternary sediments adjacent to the stream. The findings demonstrated a notable shift from low-permeability clay-dominated sediments to more permeable sands and gravels downstream within the streambed alluvium.

Using hydraulic and geophysical data sets, we develop a generalized conceptual model of the stream hydrology by way of variations in superficial geological structure around the stream explaining the complexities in surface water-groundwater dynamics. We hypothesize that two dominant controls on water balance partitioning exist:

1. The permeability contrast between recent streambed alluvium and surrounding superficial geology;
2. The volume of recent alluvium at and upstream of a given location within the catchment.

High permeability contrasts between streambed alluvium and the surrounding superficial geology controls water balance partitioning within the stream by creating an “alluvial store” of perched water within the streambed sediments that is partitioned longitudinally downstream within the alluvium. Longitudinal flow from alluvial volumes upstream manifests itself as streamflow and maintains the saturation of alluvium downstream. Where streambed alluvium intersects areas with lower permeability contrasts, alluvial water is more readily distributed away from the stream (vertically and transversely). These two controls exist as a continuum within the catchment and likely intersect in any given dryland catchment to maximize the available water within the alluvium in both space and time, creating a “goldilocks zone” that maximizes riparian water availability and groundwater recharge potential.

Our conceptual model provides a first step for improved understanding of water balance partitioning in dryland IRES. Future work should focus on the transferability of this conceptual model to other dryland catchments which have sufficient groundwater level data available, with the end goal of developing a process understanding of water balance partitioning within IRES that can be upscaled over broad areas and ungauged catchments. This would allow improved understanding of water availability and groundwater recharge under a changing climate. The work in this study emphatically underscores the imperative of considering geological controls when classifying streams according to their flow regimes.

Data Availability Statement

The data used in this paper were collected with equipment and field infrastructure (monitoring boreholes) provided by the Australian Federal Government-financed National Collaborative Research Infrastructure Strategy (NCRIS), the Cotton Catchment Communities CRC (Cotton CRC projects 2.02.03 and 2.02.21) and the school of Civil and Environmental Engineering (UNSW). The data used in the study are available via <https://doi.org/10.6084/m9.figshare.26721328> with CC BY 4.0 (E. Zarate et al., 2024). The raw NCRIS groundwater level data used in this paper is publicly available at Auscope via <https://doi.org/10.60623/y1ua83ti> with CC BY 4.0 (M. Andersen & Jensen, 2024).

Acknowledgments

We gratefully acknowledge contributions to field work and data sets from Dr Andrew McCallum, Evan Jensen, Fang Bian, Ivona Buczek, Calvin Li, Samuel McCulloch, and Hamish Studholme. We thank the following landowners for allowing access to the research sites in Maules Creek: Philip Laird, Alistair Todd, and Steve Bradshaw. E Zarate was supported by a NERC GW4+ Doctoral Training Partnership studentship from the Natural Environment Research Council [NE/L002434/1] and is thankful for the support and additional funding from CASE partner, the BGS. M. O. Cuthbert was supported by the European Community's Seventh Framework Program (FP7/2007–2013) under grant agreement 299091 and by the Natural Environment Research Council [NE/P017819/1]. G. C. Rau was supported by the National Centre for Groundwater Research and Training (NCGRT), an Australian Government initiative supported by the Australian Research Council (ARC) and the National Water Commission (NWC). E Zarate and A. M. MacDonald publish with the permission of the Director, British Geological Survey (UKRI).

References

- Abel, C., Horion, S., Tagesson, T., De Keersmaecker, W., Seddon, A. W. R., Abdi, A. M., & Fensholt, R. (2020). The human–environment nexus and vegetation–rainfall sensitivity in tropical drylands. *Nature Sustainability*, 4(1), 25–32. <https://doi.org/10.1038/s41893-020-00597-z>
- Acuña, V., Hunter, M., & Ruhí, A. (2017). Managing temporary streams and rivers as unique rather than second-class ecosystems. *Biological Conservation*, 211, 12–19. <https://doi.org/10.1016/j.biocon.2016.12.025>
- Acworth, R. I., Rau, G. C., Cuthbert, M. O., Jensen, E., & Leggett, K. (2016). Long-term spatio-temporal precipitation variability in arid-zone Australia and implications for groundwater recharge. *Hydrogeology Journal*, 24(4), 905–921. <https://doi.org/10.1007/s10040-015-1358-7>
- Acworth, R. I., Rau, G. C., Cuthbert, M. O., Leggett, K., & Andersen, M. S. (2020). Runoff and focused groundwater-recharge response to flooding rains in the arid zone of Australia. *Hydrogeology Journal*, 1–28.
- Alan Yeakley, J., Ervin, D., Chang, H., Granek, E. F., Dujon, V., Shandas, V., & Brown, D. (2016). Ecosystem services of streams and rivers. In *River science: Research and management for the 21st century* (pp. 335–352).
- Andersen, M., & Jensen, E. (2024). University of New South Wales (UNSW) raw groundwater levels data (2012–2024) [Dataset]. <https://doi.org/10.60623/y1ua83ti>
- Andersen, M. S., & Acworth, R. I. (2009). Stream-aquifer interactions in the Maules Creek catchment, Namoi Valley, New South Wales, Australia. *Hydrogeology Journal*, 17(8), 2005–2021. <https://doi.org/10.1007/s10040-009-0500-9>
- Barrett, C. (2012). *Upper Namoi groundwater source–status report 2011*. NSW Department of Primary Industries, Office of Water.
- Bauer, P., Held, R. J., Zimmermann, S., Linn, F., & Kinzelbach, W. (2006). Coupled flow and salinity transport modelling in semi-arid environments: The Shashe River Valley, Botswana. *Journal of Hydrology*, 316(1–4), 163–183. <https://doi.org/10.1016/j.jhydrol.2005.04.018>
- Berdugo, M., Delgado-Baquerizo, M., Soliveres, S., Hernández-Clemente, R., Zhao, Y., Gaitán, J. J., et al. (2020). Global ecosystem thresholds driven by aridity. *Science*, 367(6479), 787–790. <https://doi.org/10.1126/science.aay5958>
- Bourke, S. A., Degens, B., Searle, J., de Castro Tayer, T., & Rothery, J. (2021). Geological permeability controls streamflow generation in a remote, ungauged, semi-arid drainage system. *Journal of Hydrology: Regional Studies*, 38, 100956. <https://doi.org/10.1016/j.ejrh.2021.100956>
- Brown, R. E., Krynen, J. P., & Brownlow, J. W. (1992). *Manilla-Narrabri 1:250 000 Metallogenic Map* (1st ed.). Geological Survey of New South Wales.
- Brunner, P., Cook, P. G., & Simmons, C. T. (2011). Disconnected surface water and groundwater: From theory to practice. *Ground Water*, 49(4), 460–467. <https://doi.org/10.1111/j.1745-6584.2010.00752.x>
- Bull, L. J., & Kirkby, M. J. (2002). Dryland river characteristics and concepts. In *Dryland rivers: Hydrology and geomorphology of semi-arid channels* (pp. 3–15).
- Callegary, J. B., Leenhouts, J. M., Paretto, N. V., & Jones, C. A. (2007). Rapid estimation of recharge potential in ephemeral-stream channels using electromagnetic methods, and measurements of channel and vegetation characteristics. *Journal of Hydrology*, 344(1–2), 17–31. <https://doi.org/10.1016/j.jhydrol.2007.06.028>

- Carling, G. T., Mayo, A. L., Tingey, D., & Bruthans, J. (2012). Mechanisms, timing, and rates of arid region mountain front recharge. *Journal of Hydrology*, 428–429, 15–31. <https://doi.org/10.1016/j.jhydrol.2011.12.043>
- Chen, C., Park, T., Wang, X., Piao, S., Xu, B., Chaturvedi, R. K., et al. (2019). China and India lead in greening of the world through land-use management. *Nature Sustainability*, 2(2), 122–129. <https://doi.org/10.1038/s41893-019-0220-7>
- Clifford, J., & Binley, A. (2010). Geophysical characterization of riverbed hydrostratigraphy using electrical resistance tomography. *Near Surface Geophysics*, 8(6), 493–501. <https://doi.org/10.3997/1873-0604.2010035>
- Cook, P. G., O'Grady, A. P., Wischusen, J. D. H., Duguid, A., Fass, T., & Eamus, D. (2008). Ecohydrology of sand plain woodlands in central Australia.
- Costa, A. C., Foerster, S., de Araújo, J. C., & Bronstert, A. (2013). Analysis of channel transmission losses in a dryland river reach in north-eastern Brazil using streamflow series, groundwater level series and multi-temporal satellite data. *Hydrological Processes*, 27(7), 1046–1060. <https://doi.org/10.1002/hyp.9243>
- Cuthbert, M. O., Acworth, R. I., Andersen, M. S., Larsen, J. R., McCallum, A. M., Rau, G. C., & Tellam, J. H. (2016). Understanding and quantifying focused, indirect groundwater recharge from ephemeral streams using water table fluctuations. *Water Resources Research*, 52(2), 827–840. <https://doi.org/10.1002/2015WR017503>
- Cuthbert, M. O., Mackay, R., Tellam, J. H., & Barker, R. D. (2009). The use of electrical resistivity tomography in deriving local-scale models of recharge through superficial deposits. *The Quarterly Journal of Engineering Geology and Hydrogeology*, 42(2), 199–209. <https://doi.org/10.1144/1470-9236/08-023>
- Cuthbert, M. O., Taylor, R. G., Favreau, G., Todd, M. C., Shamsudduha, M., Villholth, K. G., et al. (2019). Observed controls on resilience of groundwater to climate variability in sub-Saharan Africa. *Nature*, 572(7768), 230–234. <https://doi.org/10.1038/s41586-019-1441-7>
- Dahan, O., Tatarsky, B., Enzel, Y., Kulls, C., Seely, M., & Benito, G. (2008). Dynamics of flood water infiltration and ground water recharge in hyperarid desert. *Ground Water*, 46(3), 450–461. <https://doi.org/10.1111/j.1745-6584.2007.00414.x>
- Dahlin, T., & Owen, R. (1998). Geophysical investigations of alluvial aquifers in Zimbabwe. In *Proceedings of the IV meeting of the environmental and engineering geophysical society (European section)* (pp. 151–154).
- Dai, A. (2013). Increasing drought under global warming in observations and models. *Nature Climate Change*, 3(1), 52–58. <https://doi.org/10.1038/nclimate1633>
- Datry, T., Arscott, D. B., & Sabater, S. (2011). Recent perspectives on temporary river ecology. *Aquatic Sciences*, 73(4), 453–457. <https://doi.org/10.1007/s00027-011-0236-1>
- Datry, T., Bonada, N., & Boulton, A. (2017). Intermittent rivers and ephemeral streams: Ecology and management. *Hrvatske Vode*, 25, 102.
- Datry, T., Fritz, K., & Leigh, C. (2016). Challenges, developments and perspectives in intermittent river ecology. *Freshwater Biology*, 61(8), 1171–1180. <https://doi.org/10.1111/fwb.12789>
- Datry, T., Pella, H., Leigh, C., Bonada, N., & Huguency, B. (2016). A landscape approach to advance intermittent river ecology. *Freshwater Biology*, 61(8), 1200–1213. <https://doi.org/10.1111/fwb.12645>
- DESA, U. N. (2017). *World population prospects, the 2017 revision, volume I: Comprehensive tables*. New York United Nations Department of Economic & Social Affairs.
- Dvory, N. Z., Livshitz, Y., Kuznetsov, M., Adar, E., & Yakirevich, A. (2016). The effect of hydrogeological conditions on variability and dynamic of groundwater recharge in a carbonate aquifer at local scale. *Journal of Hydrology*, 535, 480–494. <https://doi.org/10.1016/j.jhydrol.2016.02.011>
- Edwards, L. S. (1977). A modified pseudosection for resistivity and IP. *Geophysics*, 42(5), 1020–1036. <https://doi.org/10.1190/1.1440762>
- El Khalki, E. M., Trambly, Y., Massari, C., Brocca, L., Simonneaux, V., Gascoin, S., & Saidi, M. E. M. (2020). Challenges in flood modeling over data-scarce regions: How to exploit globally available soil moisture products to estimate antecedent soil wetness conditions in Morocco. *Natural Hazards and Earth System Sciences*, 20(10), 2591–2607. <https://doi.org/10.5194/nhess-20-2591-2020>
- Feng, S., & Fu, Q. (2013). Expansion of global drylands under a warming climate. *Atmospheric Chemistry and Physics*, 13(19), 10081–10094. <https://doi.org/10.5194/acp-13-10081-2013>
- Flinchum, B. A., Banks, E., Hatch, M., Batelaan, O., Peeters, L. J. M., & Pasquet, S. (2020). Identifying recharge under subtle ephemeral features in a flat-lying semi-arid region using a combined geophysical approach. *Hydrology and Earth System Sciences*, 24(9), 4353–4368. <https://doi.org/10.5194/hess-24-4353-2020>
- Fuchs, E. H., King, J. P., & Carroll, K. C. (2019). Quantifying disconnection of groundwater from managed-ephemeral surface water during drought and conjunctive agricultural use. *Water Resources Research*, 55(7), 5871–5890. <https://doi.org/10.1029/2019wr024941>
- Gleeson, T., Cuthbert, M., Ferguson, G., & Perrone, D. (2020). Global groundwater sustainability, resources, and systems in the anthropocene. *Annual Review of Earth and Planetary Sciences*, 48(1), 431–463. <https://doi.org/10.1146/annurev-earth-071719-055251>
- Godsey, S. E., & Kirchner, J. W. (2014). Dynamic, discontinuous stream networks: Hydrologically driven variations in active drainage density, flowing channels and stream order. *Hydrological Processes*, 28(23), 5791–5803. <https://doi.org/10.1002/hyp.10310>
- Goodrich, D. C., Kepner, W. G., Levick, L. R., & Wigington, P. J. (2018). Southwestern intermittent and ephemeral stream connectivity. *Journal of the American Water Resources Association*, 54(2), 400–422. <https://doi.org/10.1111/1752-1688.12636>
- Goodrich, D. C., Williams, D. G., Unkrich, C. L., Hogan, J. F., Scott, R. L., Hultine, K. R., et al. (2004). Comparison of methods to estimate ephemeral channel recharge, Walnut Gulch, San Pedro River Basin, Arizona, 77–99. <https://doi.org/10.1029/009WSA06>
- Green, T. R., Taniguchi, M., Kooi, H., Gurdak, J. J., Allen, D. M., Hiscock, K. M., et al. (2011). Beneath the surface of global change: Impacts of climate change on groundwater. *Journal of Hydrology*, 405(3–4), 532–560. <https://doi.org/10.1016/j.jhydrol.2011.05.002>
- Harrington, G. A., Gardner, W. P., & Munday, T. J. (2014). Tracking groundwater discharge to a large river using tracers and geophysics. *Groundwater Series*, 52(6), 837–852. <https://doi.org/10.1111/gwat.12124>
- Huang, J., Li, Y., Fu, C., Chen, F., Fu, Q., Dai, A., et al. (2017). Dryland climate change: Recent progress and challenges. *Reviews of Geophysics*, 55(3), 719–778. <https://doi.org/10.1002/2016RG000550>
- Huang, J., Yu, H., Guan, X., Wang, G., & Guo, R. (2016). Accelerated dryland expansion under climate change. *Nature Climate Change*, 6(2), 166–171. <https://doi.org/10.1038/nclimate2837>
- Hughes, D. A. (2008). Modelling semi-arid and arid hydrology and water resources: The southern Africa experience. In *Hydrological modelling in arid and semi-arid areas* (pp. 1–20).
- Hussey, S. W. (1997). Small-scale sand abstraction systems. In *1997 23rd WEDC international conference: Water and sanitation for all—Partnerships and innovations* (pp. 283–285). Water Workshop.
- Hvorslev, M. J. (1951). *Time lag and soil permeability in ground-water observations*. Waterways Experiment Station, Corps of Engineers, US Army.
- Jaeger, K. L., Sutfin, N. A., Tooth, S., Michaelides, K., & Singer, M. (2017). Geomorphology and sediment regimes of intermittent rivers and ephemeral streams. In *Intermittent rivers and ephemeral streams*. <https://doi.org/10.1016/b978-0-12-803835-2.00002-4>

- Jasechko, S., & Taylor, R. G. (2015). Intensive rainfall recharges tropical groundwaters. *Environmental Research Letters*, 10(12), 124015. <https://doi.org/10.1088/1748-9326/10/12/124015>
- Kaletová, T., Loures, L., Castanho, R. A., Aydin, E., da Gama, J. T., Loures, A., & Truchy, A. (2019). Relevance of intermittent rivers and streams in agricultural landscape and their impact on provided ecosystem services—A Mediterranean case study. *International Journal of Environmental Research and Public Health*, 16(15), 2693. <https://doi.org/10.3390/ijerph16152693>
- Katz, G. L., Denslow, M. W., & Stromberg, J. C. (2012). The Goldilocks effect: Intermittent streams sustain more plant species than those with perennial or ephemeral flow. *Freshwater Biology*, 57(3), 467–480. <https://doi.org/10.1111/j.1365-2427.2011.02714.x>
- Keppel, R. V., & Renard, K. G. (1962). Transmission losses in ephemeral stream beds. *Journal of the Hydraulics Division*, 88(3), 59–68. <https://doi.org/10.1061/jyceaj.0000734>
- Keshavarzi, M., Baker, A., Kelly, B. F. J., & Andersen, M. S. (2017). River–groundwater connectivity in a karst system, Wellington, New South Wales, Australia. *Hydrogeology Journal*, 25(2), 557–574. <https://doi.org/10.1007/s10040-016-1491-y>
- Koehn, W. J., Tucker-Kulesza, S. E., & Steward, D. R. (2020). Characterizing riverbed heterogeneity across shifts in river discharge through temporal changes in electrical resistivity. *Journal of Environmental & Engineering Geophysics*, 25(4), 581–587. <https://doi.org/10.32389/jeeeg20-049>
- Labbe, T. R., & Fausch, K. D. (2000). Dynamics of intermittent stream habitat regulate persistence of a threatened fish at multiple scales. *Ecological Applications*, 10(6), 1774–1791. <https://doi.org/10.2307/2641238>
- Lange, J. (2005). Dynamics of transmission losses in a large arid stream channel. *Journal of Hydrology*, 306(1–4), 112–126. <https://doi.org/10.1016/j.jhydrol.2004.09.016>
- Lange, J., Leibundgut, C., Grodek, T., Lekach, J., & Schick, A. (1998). *Using artificial tracers to study water losses of ephemeral floods in small arid streams* (Vol. 247, pp. 31–40). IAHS-AISH Publication.
- Levick, L. R., Goodrich, D. C., Hernandez, M., Fonseca, J., Semmens, D. J., Stromberg, J., et al. (2008). The ecological and hydrological significance of ephemeral and intermittent streams in the arid and semi-arid American southwest.
- Loke, M. H. (2006). RES2DINV ver. 3.55, Rapid 2-D resistivity & IP inversion using the least-squares method. *Software Manual*, 139.
- Loke, M. H., Acworth, I., & Dahlin, T. (2003). A comparison of smooth and blocky inversion methods in 2D electrical imaging surveys. *Exploration Geophysics*, 34(3), 182–187.
- Lorentz, S., Riddell, E. S., Nel, J., Van Tol, J., Fundisi, D., Jumbi, F., & van Niekerk, A. (2020). Groundwater-surface water interactions in an ephemeral savanna catchment, Kruger National Park. *Koedoe: African Protected Area Conservation and Science*, 62(2), 1–14. <https://doi.org/10.4102/koedoe.v62i2.1583>
- Love, D., van der Zaag, P., Uhlenbrook, S., & Owen, R. J. S. (2010). A water balance modelling approach to optimising the use of water resources in ephemeral sand rivers. *River Research and Applications*, 27(7), 908–925. <https://doi.org/10.1002/rra.1408>
- McCallum, A. M., Andersen, M. S., Giambastiani, B. M. S., Kelly, B. F. J., & Ian Acworth, R. (2013). River-aquifer interactions in a semi-arid environment stressed by groundwater abstraction. *Hydrological Processes*, 27(7), 1072–1085. <https://doi.org/10.1002/hyp.9229>
- McCallum, A. M., Andersen, M. S., Rau, G. C., Larsen, J. R., & Acworth, R. I. (2014). River-aquifer interactions in a semiarid environment investigated using point and reach measurements. *Water Resources Research*, 50(4), 2815–2829. <https://doi.org/10.1002/2012WR012922>
- Meixner, T., Manning, A. H., Stonestrom, D. A., Allen, D. M., Ajami, H., Blasch, K. W., et al. (2016). Implications of projected climate change for groundwater recharge in the western United States. *Journal of Hydrology*, 534, 124–138. <https://doi.org/10.1016/j.jhydrol.2015.12.027>
- Messenger, M. L., Lehner, B., Cockburn, C., Lamouroux, N., Pella, H., Snelder, T., et al. (2021). Global prevalence of non-perennial rivers and streams. *Nature*, 594(7863), 391–397. <https://doi.org/10.1038/s41586-021-03565-5>
- Moulaoum, A. W. (2018). Using field assessment and numerical modelling tools to optimize a water abstraction system in the Shashane Sand River aquifer (Zimbabwe).
- Owen, R., & Dahlin, T. (2005). Alluvial aquifers at geological boundaries: Geophysical investigations and groundwater resources. In *Groundwater and human development: International association of hydrogeologists selected papers on hydrogeology* (Vol. 6, pp. 233–246).
- Owor, M., Taylor, R. G., Tindimugaya, C., & Mwesigwa, D. (2009). Rainfall intensity and groundwater recharge: Empirical evidence from the Upper Nile Basin. *Environmental Research Letters*, 4(3), 035009. <https://doi.org/10.1088/1748-9326/4/3/035009>
- Partington, D., Shanafield, M., Banks, E. W., Andersen, M. S., Rau, G. C., Felder, S., & Simmons, C. T. (2023). Where the water goes: Partitioning surface flow and streambed infiltration in an ephemeral river laboratory experiment. *Journal of Hydrology*, 626, 130159. <https://doi.org/10.1016/j.jhydrol.2023.130159>
- Pilgrim, D. H., Chapman, T. G., & Doran, D. G. (1988). Problems of rainfall-runoff modelling in arid and semiarid regions. *Hydrological Sciences Journal*, 33(4), 379–400. <https://doi.org/10.1080/02626688809491261>
- Pool, D. R. (2005). Variations in climate and ephemeral channel recharge in southeastern Arizona, United States. *Water Resources Research*, 41(11), W11403. <https://doi.org/10.1029/2004WR003255>
- Quichimbo, E. A., Singer, M. B., & Cuthbert, M. O. (2020). Characterising groundwater–surface water interactions in idealised ephemeral stream systems. *Hydrological Processes*, 34(18), 3792–3806. <https://doi.org/10.1002/hyp.13847>
- Rassam, D. W., Fellows, C. S., De Hayr, R., Hunter, H., & Bloesch, P. (2006). The hydrology of riparian buffer zones; two case studies in an ephemeral and a perennial stream. *Journal of Hydrology*, 325(1–4), 308–324. <https://doi.org/10.1016/j.jhydrol.2005.10.023>
- Rau, G. C., Andersen, M. S., McCallum, A. M., & Acworth, R. I. (2010). Analytical methods that use natural heat as a tracer to quantify surface water–groundwater exchange, evaluated using field temperature records. *Hydrogeology Journal*, 18(5), 1093–1110. <https://doi.org/10.1007/s10040-010-0586-0>
- Rau, G. C., Halloran, L. J. S., Cuthbert, M. O., Andersen, M. S., Acworth, R. I., & Tellam, J. H. (2017). Characterising the dynamics of surface water–groundwater interactions in intermittent and ephemeral streams using streambed thermal signatures. *Advances in Water Resources*, 107, 354–369. <https://doi.org/10.1016/j.advwatres.2017.07.005>
- Rubin, Y., & Hubbard, S. S. (2006). *Hydrogeophysics* (Vol. 50). Springer Science & Business Media.
- Rutledge, H., Taschetto, A., Anderson, M., & Baker, A. (2023). Negative Indian Ocean Dipole drives groundwater recharge in southeast Australia.
- Saccò, M., Blyth, A. J., Humphreys, W. F., Cooper, S. J. B., White, N. E., Campbell, M., et al. (2021). Rainfall as a trigger of ecological cascade effects in an Australian groundwater ecosystem. *Scientific Reports*, 11(1), 1–15. <https://doi.org/10.1038/s41598-021-83286-x>
- Scott, R. L., Cable, W. L., Huxman, T. E., Nagler, P. L., Hernandez, M., & Goodrich, D. C. (2008). Multiyear riparian evapotranspiration and groundwater use for a semiarid watershed. *Journal of Arid Environments*, 72(7), 1232–1246. <https://doi.org/10.1016/j.jaridenv.2008.01.001>
- Seddou, D., Kashaigili, J. J., Taylor, R. G., Cuthbert, M. O., Mwiimbo, C., & MacDonald, A. M. (2021). Focused groundwater recharge in a tropical dryland: Empirical evidence from central, semi-arid Tanzania. *Journal of Hydrology: Regional Studies*, 37, 100919. <https://doi.org/10.1016/j.ejrh.2021.100919>

- Ségui, L., Kamagaté, B., Favreau, G., Descloitres, M., Seidel, J.-L., Galle, S., et al. (2011). Origins of streamflow in a crystalline basement catchment in a sub-humid Sudanian zone: The Donga basin (Benin, West Africa): Inter-annual variability of water budget. *Journal of Hydrology*, 402(1–2), 1–13. <https://doi.org/10.1016/j.jhydrol.2011.01.054>
- Shanfield, M., Bourke, S. A., Zimmer, M. A., & Costigan, K. H. (2021). An overview of the hydrology of non-perennial rivers and streams. *Wiley Interdisciplinary Reviews: Water*, 8(2), e1504. <https://doi.org/10.1002/wat2.1504>
- Shanfield, M., & Cook, P. G. (2014). Transmission losses, infiltration and groundwater recharge through ephemeral and intermittent streambeds: A review of applied methods. *Journal of Hydrology*, 511, 518–529. <https://doi.org/10.1016/j.jhydrol.2014.01.068>
- Shanfield, M., Gutiérrez-Jurado, K., White, N., Hatch, M., & Keane, R. (2020). Catchment-scale characterization of intermittent stream infiltration: a geophysics approach. *Journal of Geophysical Research: Earth Surface*, 125(2), e2019JF005330. <https://doi.org/10.1029/2019jfo05330>
- Shaw, J. R., & Cooper, D. J. (2008). Linkages among watersheds, stream reaches, and riparian vegetation in dryland ephemeral stream networks. *Journal of Hydrology*, 350(1–2), 68–82. <https://doi.org/10.1016/j.jhydrol.2007.11.030>
- Stromberg, J. C., & Merritt, D. M. (2016). Riparian plant guilds of ephemeral, intermittent and perennial rivers. *Freshwater Biology*, 61(8), 1259–1275. <https://doi.org/10.1111/fwb.12686>
- Stubbington, R., Acreman, M., Acuña, V., Boon, P. J., Boulton, A. J., England, J., et al. (2020). Ecosystem services of temporary streams differ between wet and dry phases in regions with contrasting climates and economies. *People and Nature*, 2(3), 660–677. <https://doi.org/10.1002/pan3.10113>
- Swenson, L. J., Zipper, S., Peterson, D. M., Jones, C. N., Burgin, A. J., Seybold, E., et al. (2024). Changes in water age during dry-down of a non-perennial stream. *Water Resources Research*, 60(1), e2023WR034623. <https://doi.org/10.1029/2023wr034623>
- Taylor, R. G., Scanlon, B., Döll, P., Rodell, M., van Beek, R., Wada, Y., et al. (2013). Ground water and climate change. *Nature Climate Change*, 3(4), 322–329. <https://doi.org/10.1038/nclimate1744>
- Taylor, R. G., Todd, M. C., Kongola, L., Maurice, L., Nahozya, E., Sanga, H., & MacDonald, A. M. (2013). Evidence of the dependence of groundwater resources on extreme rainfall in East Africa. *Nature Climate Change*, 3(4), 374–378. <https://doi.org/10.1038/nclimate1731>
- Telvari, A., Cordery, I., & Pilgrim, D. (1998). Relations between transmission losses and bed alluvium in an Australian arid zone stream. *Hydrology in a Changing Environment*, 2, 361–366.
- Villeneuve, S., Cook, P. G., Shanfield, M., Wood, C., & White, N. (2015). Groundwater recharge via infiltration through an ephemeral riverbed, central Australia. *Journal of Arid Environments*, 117, 47–58. <https://doi.org/10.1016/j.jaridenv.2015.02.009>
- Wada, Y., van Beek, L. P. H., Wanders, N., & Bierkens, M. F. P. (2013). Human water consumption intensifies hydrological drought worldwide. *Environmental Research Letters*, 8(3), 034036. <https://doi.org/10.1088/1748-9326/8/3/034036>
- Ward, A. S., Schmadel, N. M., & Wondzell, S. M. (2018). Simulation of dynamic expansion, contraction, and connectivity in a mountain stream network. *Advances in Water Resources*, 114, 64–82. <https://doi.org/10.1016/j.advwatres.2018.01.018>
- Warix, S. R., Godsey, S. E., Flerchinger, G., Havens, S., Lohse, K. A., Bottenberg, H. C., et al. (2023). Evapotranspiration and groundwater inputs control the timing of diel cycling of stream drying during low-flow periods. *Frontiers in Water*, 5, 1279838. <https://doi.org/10.3389/frwa.2023.1279838>
- Warix, S. R., Godsey, S. E., Lohse, K. A., & Hale, R. L. (2021). Influence of groundwater and topography on stream drying in semi-arid headwater streams. *Hydrological Processes*, 35(5), e14185. <https://doi.org/10.1002/hyp.14185>
- Wekesa, S. S., Stigter, T. Y., Olang, L. O., Oloo, F., Fouchy, K., & McClain, M. E. (2020). Water flow behavior and storage potential of the semi-arid ephemeral river system in the Mara Basin of Kenya. *Frontiers in Environmental Science*, 95. <https://doi.org/10.3389/fenvs.2020.00095>
- Wheater, H. (2008). Modelling hydrological processes in arid and semi-arid areas: An introduction. In *Hydrological modelling in arid and semi-arid areas* (pp. 1–20). <https://doi.org/10.1017/cbo9780511535734.002>
- Zarate, E., Cuthbert, M., Rau, G., Andersen, M. S., Acworth, I., & Macdonald, A. (2024). Open Data for “How alluvial storage controls spatiotemporal water balance partitioning in intermittent and ephemeral stream systems” [Dataset]. <https://doi.org/10.6084/m9.figshare.26721328.v2>
- Zarate, E., Hobley, D., MacDonald, A. M., Swift, R. T., Chambers, J., Kashaigili, J. J., et al. (2021). The role of superficial geology in controlling groundwater recharge in the weathered crystalline basement of semi-arid Tanzania. *Journal of Hydrology: Regional Studies*, 36, 100833. <https://doi.org/10.1016/j.ejrh.2021.100833>
- Zimmer, M. A., & McGlynn, B. L. (2017). Ephemeral and intermittent runoff generation processes in a low relief, highly weathered catchment. *Water Resources Research*, 53(8), 7055–7077. <https://doi.org/10.1002/2016wr019742>
- Zipper, S., Popescu, I., Compare, K., Zhang, C., & Seybold, E. C. (2022). Alternative stable states and hydrological regime shifts in a large intermittent river. *Environmental Research Letters*, 17(7), 074005. <https://doi.org/10.1088/1748-9326/ac7539>